

A THEORETICAL STUDY OF METEORIC TRAJECTORIES AND  
PROCESSES, INCLUDING EXAMINATION OF THE INCIDENCE  
AND CHARACTERISTICS OF PHOTOGRAPHIC METEORS BY  
REDUCTION OF ABOUT 600 DATA POINTS

By Annette Posen and Richard E. McCrosky

Distribution of this report is provided in the interest of  
information exchange. Responsibility for the contents  
resides in the author or organization that prepared it.

Prepared under Grant No. NsG-460 by  
HARVARD UNIVERSITY  
Meteor Department, Harvard College Observatory  
Cambridge, Mass.

for Lewis Research Center

NATIONAL AERONAUTICS AND SPACE ADMINISTRATION

## FOREWORD

The work described herein was performed by the Harvard College Observatory, Meteor Department, under NASA Research Grant No. NsG-460. The project director for the Harvard University was Dr. F. L. Whipple, and the Scientist-in-Charge was Dr. R. E. McCrosky. Mr. Jack F. Mondt, Space Power Systems Division, NASA-Lewis Research Center, served as Technical Manager for NASA, with technical guidance provided by Mr. S. Lieblein and Mr. C. D. Miller, both of the Fluid System Components Division, NASA-Lewis Research Center.

PRECEDING PAGE BLANK NOT FILMED.

# ABSTRACT

This report describes a newly developed, efficient, automatic-reduction procedure for photographic meteor data. The time required to process a pair of films is reduced from 24 to 3 man-hours, and this is due mainly to an electronic computer program that automatically identifies the stars on a photographic film. It is necessary to know the approximate ( $\pm 5^\circ$ ) hour angle and declination of the center of the star field of the film (the direction of the camera's optical axis) and the focal length of the camera.

This automatic star-identification technique can be widely applied to astronomical photographic data.

New, precisely computed orbits for 357 meteors are presented.

PRECEDING PAGE BLANK NOT FILMED.

## TABLE OF CONTENTS

<u>Section</u>	<u>Page</u>
ABSTRACT. . . . .	v
1 INTRODUCTION . . . . .	1
2 THE NEW TECHNIQUES . . . . .	3
2.1 General approach to meteor reduction . . . . .	3
2.2 Star identification . . . . .	4
2.3 The new approach to star identification . . . . .	5
2.4 Star identification for Super-Schmidt films . . . . .	7
2.5 The mechanics of processing . . . . .	8
3 EVALUATION OF PROCEDURE . . . . .	10
4 THE DATA. . . . .	13
5 REFERENCES . . . . .	32
<u>Appendix</u>	
A COMPUTATION OF APPROXIMATE SKY POSITION . . . . .	33
B IMPROVEMENT OF SKY COORDINATES FOR CENTER OF PLATE. . . . .	35
C COMPUTATION OF VELOCITIES AND DECELERATIONS. . . . .	36
D THE METHOD IN DETAIL . . . . .	38

PRECEDING PAGE BLANK NOT FILMED.

A THEORETICAL STUDY OF METEORIC TRAJECTORIES AND  
PROCESSES, INCLUDING EXAMINATION OF THE INCIDENCE  
AND CHARACTERISTICS OF PHOTOGRAPHIC METEORS BY  
REDUCTION OF ABOUT 600 DATA POINTS

Annette Posen<sup>1</sup> and Richard E. McCrosky<sup>2</sup>

1. INTRODUCTION

During a constant nighttime patrol, from February 1952 to January 1959, a total of 6000 meteors were simultaneously photographed by two Super-Schmidt cameras of the Harvard Meteor Project in New Mexico.

Because of the length of time required to process the films, only a limited number of precise reductions have been made in the past (Jacchia and Whipple, 1961; Hawkins and Southworth, 1961), mainly from the data collected between February 1952 and July 1954. Much of the early data was also treated in an approximate fashion ( $\pm 5\%$  in velocity) to yield a statistically significant distribution of orbits of meteoric particles (McCrosky and Posen, 1961). However, as computation of meteoroid dimensions requires very careful reduction, only the small sample of precise reductions can be used for any reliable information on this parameter.

The number, size, momentum, and energy distributions of meteoric particles in the solar system are of vital interest to designers of space vehicles.

---

<sup>1</sup>Smithsonian Astrophysical Observatory.

<sup>2</sup>Harvard College Observatory and Smithsonian Astrophysical Observatory.

We reviewed the entire reduction procedure, including the film handling and measuring process, and investigated new mathematical and logical techniques for data manipulation. We now have available precision-measuring engines with card-punch capability. Large catalogs of star positions have been compiled on magnetic tape and are thus readily accessible by electronic computer.

We developed a precise-reduction procedure of practical length, and can now base our knowledge of the distribution of meteoric particles upon a much larger sample of data.

## 2. THE NEW TECHNIQUES

### 2.1 General Approach to Meteor Reduction

The nature of the Super-Schmidt photographic data and of the results derived from them are described in detail by Whipple and Jacchia (1957).

The films are curved, conforming to the focal surface of the camera. They are photographically copied, by gnomonic projection, onto a flat glass-backed emulsion, for measuring. The cameras are driven at the sidereal rate; the meteor trails across the "stationary" star background. A great circle in the sky (the meteor trajectory) projects into a straight line on our film. The great circle is reconstructed against a background of stars seen from two known stations. Triangulation from the two stations yields ranges and heights above the mean earth for specific points along the trail. A focal-plane shutter in the camera interrupts the meteor trail to produce a time scale, and the midpoints of the segments into which the shutter chops the trailed image of the moving meteor are, in practice, the points along the trail for which coordinates are computed. A straight line is fit to these points by the method of least squares, and represents the trail in the remainder of the reduction.

The heights and distances along the trajectory are computed separately for the trail as seen from each station, because point-by-point correspondence cannot be made in the absence of an obvious "common point" in the luminosity curve. However, distances along the trail are referred to a common beginning point, the higher of the two beginning points.

Extrapolated preatmospheric velocities should match for the two plates. This velocity, with the direction and position within the atmosphere, and the date and time of encounter with the earth, serve as input data to compute the heliocentric orbit of the body.

The data that are fundamental to photographic astronomy are the precise positions of the stars photographed as a background to the event of interest. Determination of the coordinate transformation (plate constants) from plate coordinates to sky coordinates of these known stars permits the transformation of the plate coordinates of any other points on the film to known directions in space, as seen from a particular station.

## 2.2 Star Identification

The most time-consuming operation in the reduction of Super-Schmidt films has been the identification of the star field of the film. This step was followed by the selection of appropriate reference stars for measuring, catalog lookups, the manual transcription of positions, and the preparation of appropriate punched cards. This process was long, tedious, and error-prone.

The prime contribution of our project was the automation of these steps in the procedure. This accounts for the major part of the difference in time between 24 and 3 man-hours spent per meteor reduction.

The Smithsonian Astrophysical Observatory (Staff SAO, 1966) has produced a catalog of 250,000 stars that is available on magnetic tape and suitable for machine processing. Having the data in this form may enable one to eliminate printed catalog lookup from all astronomical photographic work. However, there are several levels of sophistication in possible approaches to this problem.

For example, one might simply wish to continue to identify stars in the field visually, extract their GC numbers, and search a tape ordered by GC number to find the precise position data at a standard epoch and equinox. If the number of stars of interest is small, the catalog on tape is best for a simple selection by well-established criteria. On the other hand, one could quickly organize a straightforward but inefficient tape search, where an approximate position is matched by trial and error within a long list ordered on only one coordinate at a time (e.g., Wagner, 1963).



The aim of our investigation was to eliminate completely hand reference to star charts and star catalogs and at the same time to develop within a computer an efficient reference system (more efficient than those cited above) that could be incorporated within the body of the photographic meteor-reduction procedure.

### 2.3 The New Approach to Star Identification

Given the nature of the projection of the image of the sky on the photographic plate, the focal length of the camera, the direction of the axis of the camera, and the plate coordinates of a known direction in the sky, one can compute, from the plate coordinates of an unknown star relative to the center, an approximate sky position for that star (see Appendix A).

The uncertainty in the computed position is a function of the quality of the image measured, the accuracy to which the position of the plate center is known, both on the plate and in the sky, and the uniformity of scale across the photograph. The predicted sky position must be sufficiently close to the true position of the star so that it can be matched with the appropriate catalog position. The permissible "circle of confusion" is limited by the population density of the stars in the catalog consulted and by the sensitivity of the method used to discard invalid identifications.

As Super-Schmidt films are of excellent quality, multiple- and invalid-star identifications can be easily identified by inspection of deviations from a coordinate transformation computed for two stars that gives generally good residuals when the transformation is applied to all the tentative positions assigned. Typical deviations from a plate-constants fit in the least-squares sense are of the order of  $10 \mu$  (10 arc sec).

To implement the new approach to star identification, we organized the data in the SAO Star Catalog on magnetic tape in the following form.

The stars are visualized as falling within a two-dimensional grid in right ascension and declination. The dimensions of the grid in each coordinate are established by the expected uncertainty in the prediction computation, the population density of the stars within the magnitude range being considered, and by the expected range of success in discriminating between close possibilities. A band one grid-step deep in declination comprises a  $360^\circ$  spread in right ascension, divided by an appropriate scale into rectangular grid elements. Each of these elements can be assigned a unique address, computed from its right ascension and declination, and each star can be assigned such an address, even though some multiple occupancy will occur, depending on grid size relative to population density. This grid-address codeword attached to the accurate position can be used to simulate a two-dimensional sort. The resulting tape catalog of star positions is a one-dimensional list, and can be ordered on this one variable.

However, the search-match must proceed in a circular fashion about the predicted position; therefore, an auxiliary representation is necessary. The star catalog is actually "plotted" in the computer as a series of on-or-off binary bits corresponding to occupied or unoccupied grid positions. Each of these bits has an address within the storage block that corresponds to the codewords attached to the stars. The logical operations of the computer are admirably suited to testing very quickly the condition of specific addressable bits, such as the eight grid areas surrounding the predicted position. The addresses of "on" bits are used to search later the ordered codewords on tape and extract the accurate positions of possible matches.

The general approach has wide applicability as an efficient automatic star-identification procedure, readily adaptable to a specific camera and problem.

## 2.4 Star Identification for Super-Schmidt Films

Faint stars (8th or 9th mag) are most desirable for use as fiducial points in the immediate vicinity of the meteor trail because of the generally good quality of their images, which are of optimum size for accurate measurement. The population of such faint stars in the sky is very dense. Star positions cannot be predicted on the basis of the initial data (see Appendix A) sufficiently closely to discriminate particular stars of 8th and 9th mag from their neighbors. Because we cannot identify these faint stars directly, we must use a two-stage approach to the identification of stars in the immediate vicinity of the trail.

We first prepared a plotted "map" and corresponding list (see section 2.3) for stars of 4.5 mag or brighter. Approximate positions are computed for six of these stars distributed over the plate, and these stars are identified by the process described above. The grid size for this catalog is  $1^\circ$  on a side, and the total number of stars is 820.

With the known sky coordinates of these stars and their plate coordinates relative to the center, a closer approximation to the direction of the camera axis can be computed (see Appendix B).

With this new center and the newly identified bright stars, plate constants are computed (coordinate transformation matrix from plate to sky), which can be used to predict sky coordinates of trail stars to an approximation of better than 6 arc min. This small grid size is then suitable for a search-and-match identification of the trail stars.

The grid size used for this computer plot of the stars in the sky is 6 arc min in declination and approximately (6 sec  $\delta$ ) arc min in right ascension. The scale in  $\alpha$  is not changed with every band in  $\delta$ , but sufficiently frequently to maintain reasonably equal search areas over the sky.

## 2.5 The Mechanics of Processing

For efficient use of this new form of star catalog data, the reduction procedure should no longer be thought of as a case-by-case process. If the search data are appropriately ordered, any number of predicted star positions from various unrelated plates can be matched on one sequential tape reading and a once-through match test of any segment of the catalog. This minimizes computer time per case. A compromise must be made, however, in view of several other considerations.

We do not wish to process too large a batch at any one time, for reasons other than ease of handling. If an error by the automatic card punch attached to the measuring engine, or by the man who assembles the decks, or by the computer should stop a run where work to that point is unrecoverable, it should not be allowed to waste a large amount of preparation or machine time. There is a limitation also on the length of a list of approximate positions and matched positions that can be contained in the machine with a convenient segment of the star catalog.

The entire bright-star map and list reside in the computer core at once, and a list of predicted faint-star positions is generated from this information. The faint-star map is read in so that three contiguous records reside in core ( $3^\circ$  in  $\delta$ ). The circular search can thus extend across bands in  $\delta$ . An ordered list of matched occupied map positions is compiled with case number and star number attached for later selection. The faint-star list is read sequentially,  $1^\circ$  in  $\delta$  at a time, and a list of precise positions is compiled.

This new star-identification procedure effects the major timesaving over previous methods. We also investigated every other aspect of the reduction procedure to find possible shortcuts.

Electronic computers have been used in the past to perform the arithmetic involved in the reduction, but there were always many breaks for intervention by the human computer. Human intervention is time-consuming and also error-prone, particularly in instances where tasks such as table lookup and data transcription are involved. The following "bookkeeping" operations are most readily assumed by the automatic computer: averaging of repeated measures; selection of the appropriate station coordinates for the date of the meteor (the stations were moved several times); selection of precession constants to bring the catalog star position to the equinox of the meteor year; "drawing" of the best straight line through the trail measures; applying of field corrections to trail measures (corrections derived from residuals from the plate-constants fit as a function of distance along the trail); and plotting of a retardation curve (deviation from constant velocity trajectory) to illustrate anomalies in the meteor behavior or in the measures (see Appendix C).

Measuring engines now available can be attached to automatic card-punching readout. Such a device eliminates the need for the measurer to look away from the machine repeatedly to transcribe vernier readings and then later to prepare these data into appropriately formatted punched cards. The engine screws have been motorized because the new star-identification technique requires measures over a wide area of the plate, rather than just in the vicinity of the meteor. The measuring engine used here has been fitted with a projection screen. There is less fatigue for the measurer than with the conventional eyepiece, but to suit the new conditions, new approaches had to be tried to discover the optimum density of image and focus on the copy plate in the region of the meteor.

The timesaving in incorporating such simple and uncompromising automation is very significant. See Appendix D for a step-by-step account of the procedure.

### 3. EVALUATION OF PROCEDURE

We achieved an eightfold reduction in handling time per meteor pair without loss of accuracy.

The star identification is not always successful. The reasons for this are not obvious; there is no apparent inherent reason for failure. We do have the difficulty in this data sample of greater uncertainty in the center of the field than we would like. At the time this information ( $HA_c, \delta_c$ ) was recorded, it was not anticipated that it would be used in any other way than as a guide to the appropriate region of the star chart. A further displacement of the center occurs during the copying process where the projection center is displaced from the shutter center in the attempt to optimize the focus in a particular region of the field. This can be translated only approximately into a displacement in the sky, and a new direction center-North Pole. Sometimes there is no visual observation to fit the time of the meteor, and so there is uncertainty in the hour angle of the center at the appropriate time.

There are unanticipated omissions in the catalogs. A new version has just been received, and it will be processed into the appropriate form.

The measurer cannot always judge which of the bright-appearing stars on a film are indeed brighter than visual magnitude 4.5, or 9, the limits for the two catalogs used.

The failure rate at the extreme edges of the field is unexpectedly high in view of the generally high quality of the Super-Schmidt films.

When the stars have been successfully identified, the reduction proceeds in the standard fashion, except for a few new tasks assigned to the machine. All measured trail points are included in the determination of the straight-line trajectory. When this is done visually, obvious spurious points are

omitted (e. g. , in faint regions where the scatter of the measures must be high). The curve is fitted by machine to the plate-constants deviations and is used as a field-correction curve. However, the field correction is rarely large enough to be troublesome except for very long meteors or those crossing the center of the field. The retardation curve (see Appendix C) is plotted by machine. It should be inspected for obviously misnumbered dashes (where there are faint gaps, difficult to count), or obviously bad measures, and the effects of shutter flutter and camera vibration. (See Figure C-1.) This winnowing of the dash measures was not done for our sample because these irregularities occur infrequently. However, the velocities used as orbit input were determined by careful inspection rather than directly from the derived relation between D and t along the trail (see Appendix C).

However, meteor data cannot be handled entirely in a routine fashion. Expert judgment is required at several points. Where we have made an attempt to circumvent this, we have programmed a computer plot for ready reference to judge the success of the programmed decision. Unfortunately, decisions that help to compute meaningful initial velocities and midtrajectory decelerations have not yet been successfully programmed. We are encouraged by the progress made, but are not yet prepared to apply the method to large quantities of data.

The probable errors of the velocities have been deliberately omitted since we have not yet devised a consistent and satisfactory scheme for extrapolating the observed velocity to the preatmospheric velocity required to compute the orbit. At present, all measured dashes are included in a least-squares fit to a relation between the distance D along the trail and time t :

$$D = a + bt + ce^{kt} ,$$

from which we derive

$$V_{\infty} = \left( \frac{dD}{dt} \right)_{t=-\infty} = b \quad .$$

If the meteor duration is great enough and the basic data are accurate enough, this formulation is most satisfactory. But spurious results are often obtained if these conditions are not fulfilled. It appears that the derived quantity  $D$  must be inspected to determine the best method of computing the velocity and probable errors for each individual case. Velocities were individually considered in our sample because of their importance in orbit computations. Decelerations also are not available on an automated impersonal basis for consistent computation of masses.

We have made no photometric measures on our sample of meteors, but we have tried to devise a reasonably simple impersonal method of machine densitometry, as opposed to the visual method used in the past.



#### 4. THE DATA

A total of 415 pairs of Super-Schmidt meteor camera films have been measured and reduced by our new semiautomated procedures described above. For 357 of these we were able to compute orbital elements. The remaining 14% failed at some preliminary stage of the computations, mostly for one of the following reasons:

1. The star catalog was incomplete.
2. Stars of negative declination were not identified because of an uncorrected error in the machine program.
3. Meteor trails selected as a pair were actually photographs of two different objects.
4. Meteors near the edge of the field presumably suffered from a general degradation of the star-prediction process for stars very far from the projection center and in poor focus as the extreme edge of the film is reached.

Tables 1 and 2 present the orbital and trajectory data for these 357 meteors.

Figures 1 to 5 illustrate the frequency distributions of the orbital elements  $1/a$ ,  $e$ ,  $q$ ,  $i$ , and the meteor velocity  $V_{\infty}$  used to compute the orbits. The characteristics of these distributions are similar to those obtained by McCrosky and Posen (1961) and by Hawkins and Southworth (1961), the latter indicated by solid-line plots on Figures 1 to 5.

The large number of hyperbolic cases relative to the sample of Hawkins and Southworth reflects our difficulty in selecting the appropriate  $V_{\infty}$  without the very careful examination customarily used. (See Section 3.)

The following is an explanation of column heads used in Tables 1 and 2. Orbital data are referred to Equinox 1950. 0.

film	Film number in SL camera series — always used as station A of the pair
mo/day/yr	Date and time of day in U. T. for meteor occurrence
a	Semimajor axis (a. u. )
e	Eccentricity
q	Perihelion distance (a. u. )
q'	Aphelion distance (a. u. )
$\omega$	Argument of perihelion (degrees)
$\Omega$	Longitude of ascending node (degrees)
i	Inclination of the orbit plane to the ecliptic (degrees)
c. w.	Cosmic weight (see Whipple, 1954)
$\lambda$	Elongation of the true radiant from the apex of earth's motion (degrees)
$\alpha^\circ, \delta^\circ$	True radiant of meteor, right ascension and declination (degrees)
$CZ_R$	Cosine of the zenith angle of the apparent radiant
$n_A$	Number of shutter breaks visible on the SL trail (0.0167 sec/break)
$n_{ML}$	Number of shutter break at maximum light on SL film
H BEG, END	Beginning and end heights (km) computed for the trail at each station denoted by A, B
$H_{ML}$	Height at maximum light, computed for SL trail
$\sin Q$	Q is the angle between the apparent great circles of motion as seen from the two stations
$V_\infty$	Meteor velocity (km/sec) outside earth's atmosphere
$V_G, V_H$	Meteor velocity (km/sec), relative to earth and to sun, respectively

Table 1. Meteor orbital data from Super-Schmidt double-station photographs

Film	no	day	yr	a	e	q	q'	$\omega$	$\Omega$	i	c.w.	$\lambda$	$\alpha^\circ$	$\delta^\circ$	CZ <sub>R</sub>
1866	6	8-39047	53	-7.352	1.130	0.453	>50	152.6	135.5	109.5	1.34	43.3	41.49	59.90	0.728
2855	12	13-53006	53	1.455	0.502	0.143	2.775	323.4	261.2	23.6	8.48	63.5	111.76	32.47	0.705
2855	12	13-53008	53	1.510	0.908	0.143	2.891	323.7	261.2	24.1	8.08	63.4	111.80	32.34	0.710
9234	10	4-24583	56	3.216	0.875	0.402	6.031	286.4	190.9	1.7	0.90	82.9	16.89	8.82	0.861
9285	10	10-21555	56	2.459	0.605	0.972	3.945	201.6	196.8	22.3	8.35	107.5	305.22	48.78	0.798
9287	10	10-23186	56	2.434	0.688	0.759	4.110	245.7	196.8	3.4	3.43	104.4	0.24	7.65	0.906
9298	10	10-38895	56	3.311	0.981	0.649	>50	72.9	17.0	113.2	3.52	42.9	79.61	-9.14	0.656
9298	10	10-39320	56	4.553	0.940	0.296	9.611	63.1	197.0	168.2	0.87	32.2	143.67	18.92	0.179
9305	10	10-46590	56	14.852	0.933	0.997	28.707	183.3	137.0	137.8	0.15	24.8	112.09	46.90	0.739
9305	10	10-46590	56	14.852	0.933	0.997	28.707	183.3	137.0	137.8	0.15	24.8	112.09	46.90	0.739
9308	10	11-27329	56	4.476	0.978	0.973	>50	161.8	197.8	77.8	2.03	62.7	178.63	73.36	0.286
9308	10	11-27329	56	4.476	0.978	0.973	>50	161.8	197.8	77.8	2.03	62.7	178.63	73.36	0.286
9310	10	11-27960	56	2.835	0.659	0.792	1.291	284.0	197.9	9.1	8.96	108.0	353.73	18.36	0.876
9311	10	11-30869	56	1.845	0.759	0.372	3.318	294.4	197.9	10.9	6.22	78.3	24.93	20.86	0.979
9311	10	11-31213	56	3.873	0.750	0.967	6.780	202.0	197.9	19.9	8.98	115.1	309.31	40.31	0.497
9312	10	11-31882	56	2.628	0.731	0.548	3.529	273.9	197.9	7.7	5.97	88.2	15.15	17.42	0.944
9317	10	11-37325	56	-31.290	1.011	0.350	>50	104.9	17.9	68.8	9.80	63.9	55.20	-11.77	0.710
9318	10	11-44720	56	3.273	0.759	0.787	5.758	59.3	18.0	8.5	8.28	101.1	7.98	-15.27	0.182
9319	10	11-45133	56	1.865	0.844	0.295	3.475	122.7	18.0	5.3	2.77	73.2	32.93	9.08	0.686
9321	10	11-47521	56	15.555	0.987	0.196	30.913	231.9	18.0	158.5	1.87	38.1	146.66	6.56	0.455
9321	10	11-47521	56	15.555	0.987	0.196	30.913	231.9	18.0	158.5	1.87	38.1	146.66	6.56	0.455
9327	10	12-33928	56	1.906	0.842	0.302	3.510	121.8	18.9	7.7	3.94	75.4	34.21	7.49	0.904
9328	10	12-34859	56	2.655	0.900	0.302	3.910	132.4	18.9	6.9	2.83	71.0	37.79	10.80	0.930
9333	10	12-39956	56	13.477	0.961	0.526	26.427	268.0	198.9	174.9	0.27	25.7	83.69	25.64	0.921
9342	10	15-43160	56	-13.545	1.065	0.968	>50	193.2	201.9	136.7	0.54	23.4	111.11	47.73	0.847
9343	10	15-44617	56	-80.270	1.008	0.680	>50	248.5	202.0	161.1	0.78	23.2	91.93	32.99	0.978
9343	10	15-44617	56	1.628	0.729	0.442	2.815	108.7	22.0	3.4	2.58	81.5	30.62	8.36	0.638
9345	10	15-46640	56	0.641	0.689	0.262	1.421	143.9	22.0	44.5	15.49	55.8	67.23	-9.10	0.707
9361	10	31-23528	56	2.680	0.677	0.866	4.494	227.0	217.7	5.4	5.75	116.7	4.69	17.57	0.942
9363	10	31-26157	56	7.321	0.987	0.096	14.546	145.0	37.7	37.0	8.10	64.1	64.86	10.91	0.741
9369	10	31-34308	56	3.344	0.741	0.866	5.872	45.4	37.8	12.0	10.56	113.0	22.98	-22.32	0.445
9371	10	31-36530	56	1.975	0.815	0.358	3.592	114.8	37.8	5.7	3.24	78.4	49.21	12.99	0.911
9385	11	5-28403	56	17.625	0.594	0.105	35.546	142.4	42.7	19.3	4.62	65.70	65.70	15.37	0.878
9396	11	6-30962	56	2.312	0.850	0.347	4.277	294.6	223.8	2.3	1.19	78.8	52.99	21.03	0.979
9396	11	6-31007	56	2.255	0.851	0.337	4.181	295.9	223.8	2.6	1.36	78.2	53.58	21.44	0.981
9397	11	6-31926	56	1.978	0.794	0.408	3.548	109.2	43.8	5.6	3.40	80.9	52.77	13.42	0.946
9398	11	6-32613	56	2.155	0.838	0.350	3.960	114.6	43.8	1.6	0.86	78.6	53.99	17.95	0.966
9400	11	6-33237	56	2.107	0.877	0.260	3.954	305.4	223.8	14.1	6.08	73.1	57.57	29.53	0.995
9405	11	6-38473	56	2.111	0.778	0.468	3.755	101.8	43.8	5.1	3.53	84.3	49.48	12.32	0.837
9411	11	7-30794	56	1.565	0.646	0.523	2.508	100.4	44.8	5.0	4.17	84.8	50.18	11.37	0.932
9412	11	7-31701	56	0.824	0.331	0.625	1.243	118.9	44.8	2.0	2.30	74.3	60.48	14.62	0.948
9413	11	7-32338	56	17.625	0.594	0.105	35.546	142.4	42.7	19.3	4.62	65.70	65.70	15.37	0.878
9432	11	7-48410	56	12.806	0.993	0.120	33.937	319.9	224.8	2.0	0.56	65.0	110.77	22.12	0.978
9438	11	9-31095	56	2.519	0.660	0.856	4.182	288.9	46.8	4.0	4.54	115.6	23.92	-1.64	0.888
9446	11	9-37972	56	0.974	0.114	0.863	1.085	284.9	226.9	2.8	1.03	79.9	48.83	45.26	0.895
9452	11	9-37972	56	3.500	0.851	0.520	6.480	88.1	226.9	135.5	2.45	32.6	173.61	24.39	0.199
9452	11	9-42507	56	11.414	0.536	0.730	22.097	62.7	46.9	176.2	0.14	18.1	121.46	18.28	0.896
9466	11	10-34564	56	2.187	0.800	0.437	3.936	105.8	49.8	5.4	3.41	82.9	56.79	14.23	0.922
9469	11	10-37730	56	6.238	0.883	0.727	11.749	64.2	49.9	169.3	0.38	18.6	123.89	14.16	0.783
9472	11	11-39846	56	1.741	0.659	0.525	2.958	98.1	48.9	5.2	4.24	85.9	53.12	12.10	0.783
9478	11	12-44666	56	-608.366	1.000	0.294	>50	293.9	229.9	141.8	2.99	38.8	106.91	36.10	0.998
9487	11	14-42642	56	2.211	0.859	0.355	4.666	292.9	231.9	2.7	1.43	78.5	60.72	22.99	0.801
9488	11	14-43412	56	2.246	0.837	0.366	4.125	297.6	231.9	2.9	1.63	78.6	60.56	23.30	0.777
9491	11	22-08197	56	1.754	0.476	0.940	2.649	211.6	239.7	14.2	10.12	112.5	354.00	53.58	0.927
9503	11	27-19204	56	2.551	0.641	0.889	4.213	41.4	64.8	12.7	10.66	113.2	45.85	-18.95	0.590
9503	11	27-19315	56	62.640	0.598	0.120	>50	139.4	64.8	24.9	5.92	67.5	88.03	15.15	0.803
9504	11	27-20508	56	3.866	0.698	0.396	7.336	105.3	54.8	4.6	2.27	82.6	71.95	18.33	0.803
9511	11	27-22637	56	2.606	0.826	0.359	3.761	294.3	245.0	1.4	0.79	78.6	75.63	24.05	0.988
9513	11	27-35407	56	3.751	0.755	0.918	6.593	32.9	65.0	16.5	11.83	114.9	44.00	-29.26	0.261
9521	11	25-27738	56	44.554	0.598	0.110	>50	141.1	67.0	23.4	5.62	67.1	90.61	15.98	0.905

Table 1 (Cont.)

Film	mo	day	yr	a	e	q	q'	$\omega$	$\Omega$	i	c.w.	$\lambda$	$\alpha^\circ$	$\delta^\circ$	CZ <sub>R</sub>
9522	11	29.30467	56	2.664	C.918	C.218	5.109	128.8	67.0	17.4	6.21	71.2	86.48	13.84	0.922
9530	11	31.24662	56	1.862	C.659	C.635	0.089	264.2	248.9	4.4	3.96	92.5	83.71	28.56	0.980
9542	12	1.40836	56	-3.551	1.026	C.921	>50	209.5	249.1	117.6	1.37	37.8	165.76	45.59	0.734
9542	12	1.40836	56	1.026	C.934	C.495	0.992	170.8	69.1	173.0	-0.11	45.7	138.85	-32.42	0.344
9548	12	1.46289	56	17.022	C.942	C.985	33.058	357.3	68.2	171.0	0.07	5.3	159.75	2.89	0.767
9560	12	3.27699	56	1.612	C.777	C.359	2.866	117.0	71.0	14.3	7.68	75.8	86.08	10.71	0.878
9564	12	3.31007	56	-20.744	1.009	C.193	>50	126.9	71.0	20.5	5.70	72.5	89.29	14.17	0.935
9566	12	3.32396	56	2.124	C.758	C.514	3.734	276.3	251.0	8.6	6.00	86.0	73.03	33.05	0.989
9568	12	3.34341	56	-42.633	1.003	C.124	>50	138.2	71.1	24.0	5.85	68.1	93.79	15.26	0.952
9568	12	3.35668	56	9.033	C.972	C.254	17.812	120.2	71.1	1.7	0.62	76.2	84.96	22.36	0.970
9573	12	3.42808	56	-27.241	1.008	C.286	>50	114.5	251.2	130.9	3.91	41.7	121.38	3.24	0.869
9578	12	3.47155	56	1.326	C.885	C.147	2.505	323.9	251.2	23.2	8.34	63.0	100.94	33.78	0.872
9579	12	3.47674	56	18.972	C.951	C.924	37.019	209.2	251.2	70.4	3.95	67.3	187.28	72.88	0.680
9580	12	3.48245	56	-318.658	1.000	C.138	>50	136.0	71.2	23.1	6.02	68.9	93.14	14.98	0.692
9581	12	3.49207	56	3.851	C.829	C.667	7.115	253.4	251.2	21.9	13.04	92.1	60.49	51.83	0.480
9581	12	3.49207	56	2.265	C.853	C.325	4.093	297.3	251.2	3.3	1.72	77.1	84.00	25.94	0.609
9584	12	3.51580	56	15.616	C.941	C.928	30.303	208.3	251.2	156.5	0.41	15.8	160.31	22.74	0.980
9590	12	4.44044	56	10.248	C.905	C.979	19.557	170.3	252.2	110.7	0.81	40.8	187.78	41.80	0.661
9590	12	4.44176	56	1.551	C.540	C.070	3.067	217.2	252.2	19.0	12.87	104.9	11.97	65.44	0.346
9595	12	4.48469	56	1.310	C.947	C.070	2.550	155.6	252.2	27.7	7.86	57.7	105.69	14.74	0.792
9596	12	4.48937	56	3.371	C.734	C.896	5.846	218.3	252.2	17.1	12.63	110.9	20.57	55.32	0.179
9597	12	4.50492	56	2.767	C.790	C.568	4.846	267.7	252.2	12.7	8.85	85.2	69.67	38.52	0.451
9597	12	4.50219	56	2.142	C.589	C.880	3.403	224.6	252.2	101.7	2.29	44.3	170.62	50.78	0.911
9606	12	8.26027	56	1.061	C.860	C.148	1.973	326.8	256.1	21.3	8.15	60.7	109.33	33.03	0.800
9606	12	8.26146	56	2.141	C.595	C.867	3.415	46.8	70.1	1.2	1.39	116.5	48.47	14.30	0.914
9612	12	11.32555	56	1.437	C.902	C.141	2.569	323.8	259.2	24.6	8.10	63.1	110.03	33.62	0.970
9615	12	11.35014	56	1.356	C.894	C.144	2.569	324.1	259.2	23.5	8.04	62.9	110.23	32.82	0.989
9616	12	11.35766	56	1.455	C.434	C.846	2.143	237.6	259.2	16.0	14.10	97.9	53.30	63.74	0.724
9618	12	11.37214	56	45.619	C.583	C.847	>50	44.1	79.2	144.5	0.95	24.1	149.97	-8.63	0.550
9621	12	11.39393	56	1.441	C.500	C.144	2.738	321.4	259.2	24.8	8.25	63.2	109.98	33.21	0.996
9623	12	11.40695	56	20.087	C.951	C.984	39.189	1.2	79.3	168.4	0.09	6.8	167.37	-1.92	0.565
9624	12	11.41310	56	-27.324	1.012	C.341	>50	107.4	79.3	169.6	0.72	32.7	138.37	11.88	0.909
9629	12	11.44678	56	1.265	C.895	C.146	2.633	323.5	259.3	24.0	8.32	63.1	110.12	33.09	0.933
9634	12	12.36390	56	7.559	C.586	C.911	15.088	212.8	260.2	95.9	2.35	50.1	181.29	53.11	0.565
9638	12	12.39112	56	1.316	C.890	C.145	2.487	324.2	260.3	23.4	8.18	62.7	111.66	32.75	0.997
9641	12	12.42000	56	1.382	C.895	C.145	2.620	323.6	260.3	23.1	8.03	63.2	111.08	32.58	0.974
9659	12	13.41486	56	1.617	C.915	C.138	3.097	323.2	261.3	24.0	7.74	63.8	111.40	32.19	0.978
9658	12	13.41255	56	1.422	C.895	C.144	2.701	323.5	261.3	23.0	7.88	63.4	111.97	32.29	0.982
9659	12	13.42132	56	2.255	C.961	C.088	4.362	149.2	81.3	22.2	6.04	62.5	109.92	15.31	0.913
9660	12	13.42852	56	1.433	C.901	C.141	2.724	323.8	261.3	25.9	8.58	62.9	112.81	33.18	0.965
9660	12	13.42563	56	1.832	C.896	C.191	3.473	134.9	81.3	27.1	9.20	66.8	105.35	8.97	0.833
9660	12	13.42773	56	-3.866	1.019	C.073	>50	326.6	261.3	50.8	8.31	62.9	112.53	32.31	0.965
9661	12	13.43520	56	1.326	C.891	C.145	2.507	324.2	261.3	22.6	8.02	62.8	112.62	32.28	0.955
9661	12	13.43727	56	3.618	C.967	C.120	7.099	321.9	261.3	19.7	5.53	66.2	107.94	29.54	0.925
9671	12	13.50600	56	1.392	C.856	C.144	2.639	323.7	261.4	23.2	8.15	63.2	112.36	32.40	0.782
9671	12	13.50640	56	1.464	C.903	C.142	2.785	323.5	261.4	23.6	8.09	63.4	112.07	32.39	0.776
9671	12	13.50336	56	7.346	C.874	C.925	13.767	150.6	261.4	67.2	4.15	68.7	233.30	48.74	0.547
9672	12	13.51115	56	5.042	C.946	C.271	9.852	119.3	81.4	128.7	0.97	40.9	131.63	0.08	0.744
9672	12	13.51320	56	13.523	C.931	C.915	26.891	328.7	81.4	132.7	0.97	28.6	170.72	-25.33	0.517
9673	12	13.51645	56	3.779	C.329	C.522	1.035	26.6	261.4	5.2	2.81	48.7	221.17	1.80	0.465
9675	12	14.45756	56	45.921	C.886	C.642	>50	287.4	82.4	170.0	0.42	21.7	190.75	-10.00	0.453
9675	12	14.45507	56	1.420	C.900	C.142	2.698	323.8	262.4	23.0	7.92	63.2	113.31	32.04	0.919
9684	12	14.51940	56	10.304	C.905	C.981	19.628	173.4	252.4	-90.0	1.24	53.8	206.43	48.71	0.815
9684	12	14.51655	56	4.566	C.580	C.807	>50	129.5	262.4	153.7	0.78	20.8	193.05	4.83	0.817
9688	12	21.09452	56	4.566	C.618	C.984	4.167	180.2	269.1	9.5	5.00	139.6	340.28	36.01	0.854
9698	12	22.15607	56	5.312	C.623	C.939	9.684	205.8	270.2	52.9	5.55	79.0	219.22	75.63	0.308
9700	12	22.17647	56	3.410	C.774	C.771	6.050	239.7	270.2	42.5	11.54	81.9	125.42	75.62	0.573
9705	12	27.23268	56	1.064	C.207	C.844	1.283	260.4	275.4	1.4	1.13	92.5	93.37	30.41	0.958
9705	12	27.23536	56	2.812	C.478	C.905	4.719	216.6	275.4	23.0	12.59	103.0	47.63	75.11	0.716
9707	12	27.25451	56	1.142	C.185	C.910	1.334	237.9	275.4	5.5	3.64	101.2	78.09	55.95	0.918

Table 1 (Cont.)

Film	mo	day	yr	a	e	q	q'	$\omega$	$\Omega$	i	c.w.	$\lambda$	$\alpha^\circ$	$\delta^\circ$	CZ <sub>R</sub>
9723	12	27-36678	56	5.817	C.971	0.284	19.350	116.3	95.5	140.4	3.07	38.1	147.00	-1.35	0.790
9723	12	27-38545	56	1.762	C.710	0.512	3.013	279.1	275.5	4.2	3.17	84.8	102.26	28.24	0.920
9727	12	28-27771	56	2.068	C.798	0.418	3.717	280.3	276.4	2.8	1.65	81.2	107.01	25.34	0.963
9731	12	28-31007	56	2.491	C.607	C.978	4.004	189.8	276.5	39.7	4.89	87.4	259.86	71.64	0.265
9732	12	28-31907	56	2.101	C.792	0.437	3.765	104.8	96.5	4.6	2.82	82.1	105.17	17.92	0.968
9734	12	28-33943	56	2.117	C.572	C.907	3.327	38.1	96.5	9.4	9.48	116.9	68.33	-8.31	0.509
9737	12	28-35817	56	3.021	C.753	0.746	5.295	244.0	276.5	19.1	13.15	96.6	88.08	56.03	0.844
9737	12	28-36051	56	1.163	C.753	C.288	2.039	130.3	96.5	6.5	3.79	69.7	117.93	15.42	0.955
9739	12	28-38782	56	2.120	C.748	0.533	3.706	274.0	276.5	4.9	3.60	87.1	100.84	29.27	0.900
9744	12	28-43015	56	11.384	C.917	C.938	21.828	155.0	276.6	153.7	0.41	16.7	190.74	8.28	0.582
9768	12	30-36702	56	16.101	C.978	C.353	31.849	107.3	98.6	52.3	10.75	69.1	118.56	-8.53	0.750
9774	12	30-41915	56	1.318	C.368	0.833	1.803	244.4	278.6	12.7	12.51	96.1	91.63	60.81	0.720
9780	12	30-46839	56	41.273	C.985	0.628	2.725	254.3	278.7	34.5	12.19	85.6	112.62	54.32	0.740
9781	12	30-47674	56	1.724	C.581	C.723	7.73	73.7	98.7	10.8	10.98	95.1	92.97	2.05	0.282
9784	12	30-50228	56	4.866	C.830	0.826	8.906	229.7	278.7	132.4	1.43	29.6	184.82	25.97	0.980
9784	12	30-50266	56	1.754	C.970	0.052	3.457	157.4	98.7	20.2	5.22	58.6	131.38	13.15	0.725
9787	12	30-52517	56	25.282	C.969	0.786	49.778	53.6	98.7	132.7	1.63	30.9	160.91	-19.28	0.563
9794	1	5-21932	57	14.228	C.983	0.245	28.212	301.0	284.5	72.9	9.26	59.6	150.46	38.80	0.538
9814	1	12-46900	57	0.830	C.723	C.230	1.430	325.8	291.9	10.4	6.46	59.4	148.19	22.11	0.901
9826	1	21-10174	57	1.050	C.102	C.980	1.201	198.0	300.7	1.8	0.22	128.4	64.86	54.49	0.912
9831	1	21-114307	57	2.871	C.765	0.676	5.067	73.8	120.7	9.8	7.23	95.9	113.49	5.97	0.627
9833	1	21-11575	57	2.361	C.876	0.292	4.431	300.5	300.8	5.8	2.47	75.0	139.22	20.13	0.471
9833	1	21-11575	57	2.443	C.962	C.092	4.794	328.0	300.8	18.9	4.98	63.0	151.92	17.87	0.295
9841	1	21-123443	57	2.656	C.643	C.947	4.364	205.5	300.8	11.2	8.63	123.8	67.45	59.86	0.828
9851	1	25-19096	57	1.116	C.132	0.969	1.264	30.3	124.9	6.8	2.20	105.4	93.33	-33.75	0.400
9857	1	25-24015	57	5.901	C.872	0.756	11.046	59.9	124.9	13.4	9.47	102.4	109.28	-0.92	0.829
9863	1	32-23518	57	2.876	C.780	C.632	5.120	79.5	132.0	6.5	4.75	93.6	127.84	9.18	0.879
9901	2	1-44094	57	128.640	C.592	C.979	>50	9.5	132.2	161.5	0.17	11.0	213.11	-24.76	0.443
9920	2	6-35668	57	5.566	C.850	0.833	10.300	228.0	317.2	81.3	4.41	58.4	216.54	41.21	0.697
9923	2	6-38540	57	6.227	C.859	C.879	11.493	220.0	317.2	163.5	0.36	13.8	216.54	-5.00	0.525
9934	2	6-51686	57	-27.762	C.1014	C.538	>50	95.6	317.4	90.0	6.13	55.0	270.73	1.61	C.614
9934	2	6-17992	57	C.757	C.350	C.518	1.075	326.3	317.4	49.2	7.48	55.9	220.47	34.93	0.993
9952	2	9-45330	57	1.164	C.445	0.645	1.682	277.1	320.3	16.0	14.10	81.8	164.26	39.17	0.892
9958	2	9-51467	57	1.588	C.917	0.132	3.045	144.2	140.4	3.1	1.12	64.2	166.25	4.43	0.554
10001	2	25-36764	57	1.859	C.945	C.104	3.694	327.3	336.4	9.5	2.86	61.2	183.68	2.08	0.859
10002	2	25-38125	57	1.385	C.286	C.985	1.781	186.3	336.4	11.8	3.78	113.7	72.13	87.52	0.523
10007	2	25-42578	57	14.787	C.593	0.104	29.469	322.8	336.5	158.1	2.28	42.2	203.79	-4.54	0.798
10029	2	26-42607	57	1.701	C.472	0.859	2.504	224.7	337.5	14.8	11.96	104.2	160.60	55.13	0.794
10032	2	27-17287	57	2.331	C.575	C.990	3.671	178.0	338.2	3.0	1.36	165.1	63.06	36.30	0.754
10039	2	27-22839	57	2.234	C.622	C.852	3.656	49.8	158.3	0.2	0.24	111.9	137.87	15.62	0.953
10061	3	5-18280	57	2.142	C.556	C.094	4.189	328.4	344.2	7.1	1.98	63.0	190.52	-1.99	0.306
10075	3	5-34695	57	1.202	C.372	C.754	1.649	83.3	164.4	9.2	9.93	89.7	155.99	-15.36	0.590
10082	3	5-42169	57	3.629	C.870	C.471	6.787	97.4	164.5	134.6	2.76	33.8	216.19	-34.86	0.381
10111	3	9-36266	57	2.056	C.647	C.739	3.453	249.5	348.4	8.8	7.99	97.9	167.59	23.32	0.921
10111	3	9-35750	57	1.938	C.818	0.352	3.523	295.8	348.4	4.1	2.15	76.8	182.08	2.87	0.859
10111	3	9-35797	57	4.611	C.806	0.894	8.328	140.9	348.4	83.6	3.40	57.2	278.65	30.27	0.283
10116	3	9-40515	57	1.672	C.997	C.647	>50	232.5	348.5	143.5	1.63	28.8	236.66	-1.55	0.725
10116	3	9-43572	57	2.186	C.957	C.093	4.278	148.5	168.5	9.3	2.68	62.9	192.40	-9.58	0.670
10176	3	26-25493	57	2.771	C.826	0.483	5.060	278.1	5.2	3.6	2.06	84.9	190.13	-0.26	0.787
10188	3	28-26027	57	1.374	C.564	0.599	2.149	276.3	7.2	6.0	5.27	85.4	193.79	4.49	0.829
10192	3	28-35900	57	2.553	C.934	C.169	4.938	316.1	7.3	10.6	3.51	68.1	208.04	-6.31	0.777
10244	4	5-44253	57	-3.556	1.193	C.762	>50	235.6	15.3	87.2	4.73	57.6	251.83	24.75	0.988
10244	4	5-44579	57	2.409	C.616	0.924	3.894	143.1	15.3	61.0	4.95	70.1	298.26	46.44	0.563
10245	4	5-45497	57	2.594	C.688	0.290	4.899	300.7	15.3	8.5	3.71	74.7	209.72	-5.98	0.767
10254	4	6-42513	57	4.860	C.856	C.698	9.021	249.9	16.2	14.1	9.45	96.7	195.86	15.80	0.710
10257	4	8-36039	57	-43.523	1.023	C.981	>50	196.5	18.2	118.6	0.67	36.7	278.83	13.12	0.544
10260	4	8-39390	57	2.273	C.627	C.758	3.789	67.0	198.2	11.6	10.40	98.5	178.42	-22.95	0.250
10265	4	8-44287	57	10.515	0.516	C.688	20.150	220.4	18.2	127.4	1.34	26.6	306.73	-0.42	0.828
10270	4	10-43190	57	51.009	C.592	C.756	>50	120.5	70.2	145.4	1.25	26.6	306.73	-0.42	0.427
10270	4	10-43323	57	1.664	C.571	0.715	2.614	77.9	200.2	3.2	3.39	95.1	190.59	-11.32	0.335

Table 1 (Cont.)

Film	no	day	yr	a	e	q	q'	$\omega$	$\Omega$	i	c.w.	$\lambda$	$\alpha^\circ$	$\delta^\circ$	CZ R
10273	4	10.46509	57	5.432	0.834	0.900	9.976	140.9	20.2	100.3	2.34	47.4	299.02	24.70	0.826
10332	5	9.38933	57	1.773	0.461	0.956	2.591	213.9	48.4	21.0	9.54	101.6	228.98	44.54	0.888
10335	5	9.42127	57	1.221	0.187	0.992	1.449	152.9	68.4	28.6	2.96	85.0	292.51	67.03	0.805
10404	5	30.22695	57	15.530	0.936	0.993	30.066	196.6	68.4	35.4	2.93	98.8	246.46	54.15	0.888
10516	6	21.23558	57	11.059	0.909	1.013	21.185	173.4	90.4	83.6	-0.20	58.6	330.61	53.29	0.500
10518	6	22.23467	57	42.924	0.976	1.016	>50	179.5	90.5	77.8	-0.29	63.2	322.24	55.19	0.631
10531	6	22.26778	57	4.325	0.843	0.678	7.973	74.3	275.2	6.2	4.57	98.2	266.28	32.61	0.423
10562	6	28.41376	57	3.139	0.843	0.494	5.784	277.1	96.3	43.6	13.13	74.3	291.30	13.25	0.848
10564	6	28.43725	57	15.671	0.942	0.916	30.425	142.8	96.3	158.5	0.42	16.3	11.19	17.93	0.743
10569	7	4.25689	57	-476.632	1.002	0.962	>50	206.8	101.9	47.3	5.13	86.8	280.38	49.13	0.948
10571	7	4.27570	57	1.290	0.220	1.006	1.573	160.6	101.9	13.3	-0.15	106.6	211.80	67.21	0.642
10608	8	8.45163	57	16.535	0.938	1.012	31.658	4.4	315.5	146.9	-0.04	19.4	47.67	-2.37	0.675
10773	8	24.43184	57	2.060	0.624	0.774	3.346	248.1	330.9	3.7	4.08	103.7	322.77	-23.00	0.193
10781	8	3.31624	57	2.833	0.705	0.746	4.319	248.1	160.4	1.0	1.03	103.4	329.36	-10.38	0.683
10785	8	3.35790	57	2.916	0.837	0.475	5.357	278.9	160.5	0.4	0.25	96.5	345.87	-5.60	0.743
10785	8	3.36042	57	1.978	0.652	0.689	3.267	258.7	160.5	2.9	2.98	97.0	334.22	-5.07	0.673
10786	8	3.37433	57	1.977	0.856	0.284	3.671	303.9	160.5	6.5	3.25	74.8	354.99	2.99	0.837
10793	8	3.43676	57	1.969	0.908	0.181	3.758	136.4	340.6	33.2	10.70	66.1	11.87	-11.53	0.814
10802	9	4.36747	57	4.416	0.990	0.990	7.842	196.5	161.4	83.9	1.08	57.2	23.19	73.32	0.750
10804	9	4.39131	57	-8.224	1.109	0.898	>50	217.5	161.5	151.7	0.63	20.6	52.89	35.64	0.873
10808	9	4.43257	57	2.776	0.894	0.294	5.258	299.7	161.5	0.4	0.21	77.0	355.67	-1.55	0.655
10824	9	5.42945	57	0.856	0.503	0.702	1.010	173.8	342.5	0.3	11.85	81.9	0.93	-21.39	0.430
10825	9	5.43975	57	1.168	0.623	0.745	1.756	105.5	162.5	154.6	-0.01	14.6	71.57	36.98	0.873
10828	9	6.45417	57	0.779	0.623	0.294	1.264	327.8	163.5	9.5	8.32	57.4	11.79	17.45	0.853
10829	9	6.46110	57	-61.980	1.012	0.733	>50	117.3	163.5	167.0	0.48	19.6	93.20	30.14	0.753
10849	9	14.15208	57	2.971	0.685	0.935	5.007	214.3	171.0	20.0	10.94	109.4	304.99	33.71	0.999
10874	9	17.18034	57	1.890	0.765	0.444	3.335	106.7	353.9	4.8	3.09	82.6	4.06	-3.81	0.506
10877	9	17.21544	57	2.607	0.634	0.955	4.259	209.3	173.9	14.3	9.13	119.0	302.07	25.47	0.918
10890	9	18.27040	57	0.582	0.191	0.794	1.170	72.2	175.0	15.4	10.33	78.8	188.52	53.28	-0.041
10893	9	18.34595	57	1.746	0.822	0.311	3.180	302.0	175.0	5.1	2.78	75.5	8.01	7.83	0.904
10894	9	18.35825	57	18.550	0.953	0.875	36.225	42.6	355.1	147.4	0.81	22.6	73.14	4.29	0.538
10905	9	19.15970	57	1.694	0.821	0.303	3.085	123.3	355.8	6.9	3.55	74.8	13.13	-0.23	0.363
10909	9	20.26594	57	3.468	0.913	0.300	6.636	118.0	356.9	16.7	6.81	76.5	15.12	-5.84	0.697
10947	9	20.34598	57	2.974	0.681	0.949	4.999	210.2	177.0	30.5	9.46	97.6	305.86	51.93	0.585
10951	9	20.40208	57	3.045	0.897	0.312	5.777	297.2	177.1	6.0	2.88	78.0	7.50	8.01	0.798
10956	9	20.45262	57	-400.923	1.002	0.985	>50	195.7	177.1	124.9	0.51	33.0	77.35	55.53	0.887
10980	9	27.26260	57	2.154	0.763	0.519	3.869	96.5	3.8	6.9	4.90	87.2	10.29	-4.73	0.765
10982	9	27.28530	57	2.453	0.691	0.757	4.149	246.3	183.8	12.4	11.05	100.8	343.89	18.84	0.931
10988	9	27.34643	57	4.082	0.854	0.598	7.566	262.9	183.9	18.0	11.02	90.9	354.17	21.97	0.877
10992	9	27.41007	57	-46.756	1.016	0.751	>50	239.8	183.9	157.8	0.80	22.1	73.27	34.30	0.927
10993	9	28.20753	57	3.169	0.790	0.667	5.671	256.0	184.7	1.0	0.85	98.5	356.76	0.35	0.787
11006	9	28.23646	57	15.251	0.957	0.654	29.847	253.1	184.7	6.4	4.36	99.7	352.69	6.62	0.896
11007	9	28.24357	57	1.546	0.840	0.604	2.845	130.6	4.7	6.5	3.13	71.4	24.18	5.34	0.729
11015	9	28.33212	57	1.545	0.609	0.604	2.487	92.8	4.8	6.9	2.38	89.4	7.41	-1.07	0.812
11015	9	28.33217	57	2.487	0.768	0.577	4.396	268.6	184.8	2.9	5.31	91.1	0.60	10.30	0.877
11035	9	30.44346	57	12.190	0.919	0.986	23.394	14.3	6.9	177.5	0.02	4.7	93.68	21.94	0.462
11037	10	0.47544	57	3.082	0.870	0.400	5.764	106.9	8.8	7.1	4.00	92.4	16.79	0.23	0.862
11040	10	2.33661	57	1.323	0.603	0.525	2.122	105.3	8.8	2.6	2.47	84.2	16.73	13.94	0.711
11042	10	2.36245	57	32.137	0.978	0.710	>50	65.6	8.8	162.2	0.69	21.8	79.66	13.26	0.711
11042	10	2.36428	57	1.846	0.879	0.222	3.469	131.4	8.8	7.6	3.37	71.3	28.17	6.64	0.894
11044	10	2.38415	57	1.378	0.318	0.940	1.816	301.9	188.8	1.4	1.21	123.8	34.69	-37.41	0.287
11052	10	2.46295	57	-27.011	1.009	0.233	>50	301.9	188.9	113.9	6.08	48.1	46.73	37.70	0.936
11052	10	2.46458	57	2.355	0.861	0.465	6.245	99.0	8.9	68.6	10.16	62.8	53.82	-19.87	0.568
11052	10	2.46458	57	2.400	0.871	0.309	4.491	119.0	8.9	6.4	3.25	77.0	22.97	4.45	0.590
11052	10	2.46458	57	2.400	0.871	0.309	4.491	119.0	8.9	6.4	3.25	77.0	22.97	4.45	0.590
11075	10	17.27681	57	24.284	0.559	0.996	47.572	177.5	203.5	60.2	1.25	75.9	235.88	76.42	0.364
11075	10	17.27681	57	1.841	0.658	0.265	3.053	265.9	203.5	59.4	10.40	66.5	36.66	66.33	0.815
11093	10	24.28855	57	14.745	0.588	0.182	29.308	130.0	30.5	5.6	1.76	72.8	46.89	14.88	0.917
11093	10	24.28855	57	3.112	0.785	0.668	5.556	255.3	210.5	6.2	5.20	97.9	17.81	14.19	0.953
11096	10	24.31730	57	-16.186	1.032	0.522	>50	86.3	30.5	156.0	1.30	29.5	93.90	12.50	0.611

Table 1 (Cont.)

Film	mo	day	yr	a	e	q	q'	$\omega$	$\Omega$	i	c.w.	$\lambda$	$\alpha^\circ$	$\delta^\circ$	CZR
11111	1C	25-21318	57	2.692	C.655	C.925	4.440	214.8	211.4	1.2	1.24	130.6	350.70	0.43	0.825
11111	1C	25-21763	57	2.343	C.535	C.972	3.714	200.3	211.4	12.5	7.55	125.1	319.42	23.38	0.785
11113	1C	25-23792	57	1.973	C.818	C.359	3.586	114.8	31.4	4.6	2.52	78.6	42.56	12.14	0.828
11123	1C	25-34235	57	3.841	C.864	C.518	7.205	91.9	31.5	163.4	0.94	25.9	97.92	15.26	0.694
11127	1C	25-38052	57	-223.764	1.002	C.558	>50	82.9	31.6	163.4	0.84	26.5	97.33	15.68	0.821
11182	11	14-24717	57	3.066	C.742	C.791	5.341	236.1	231.5	10.8	9.72	105.8	24.17	33.83	0.866
11201	11	20-14445	57	1.403	C.300	C.982	1.824	193.6	237.4	17.3	6.08	104.8	307.28	60.83	0.692
11201	11	20-20052	57	103.851	C.918	C.918	>50	211.0	237.5	1.8	10.61	117.9	356.67	45.23	0.908
11208	11	20-21422	57	3.315	C.888	C.372	6.267	108.8	57.5	1.4	0.70	81.1	65.46	20.31	0.827
11213	11	20-26290	57	3.072	C.679	C.985	5.159	187.2	237.6	29.8	5.57	100.2	295.12	62.85	0.334
11215	11	20-28750	57	13.770	C.988	C.169	27.372	132.0	57.6	14.3	4.17	71.2	76.68	16.66	0.909
11221	11	20-34635	57	2.232	C.795	C.478	4.186	99.5	57.6	4.3	2.87	85.3	61.99	16.05	0.930
11224	11	20-37987	57	5.572	C.823	C.987	10.157	183.0	237.7	136.6	0.33	25.0	159.67	35.68	0.540
11227	11	21-25751	57	2.275	C.756	C.557	4.002	90.8	58.6	14.3	9.43	87.4	63.38	2.78	0.831
11256	11	23-28781	57	2.155	C.761	C.516	3.795	96.0	60.6	5.0	3.58	86.8	63.71	14.97	0.952
11282	11	25-28897	57	1.315	C.516	C.111	2.519	329.0	242.6	19.1	6.30	61.3	92.53	30.90	0.897
11284	11	25-30430	57	1.316	C.250	C.987	1.646	177.5	242.7	161.7	0.09	9.6	158.93	19.24	0.149
11284	11	25-31205	57	3.429	C.807	C.661	6.198	74.9	62.7	6.3	5.05	97.5	55.70	9.76	0.895
11290	11	25-36765	57	-42.874	1.002	C.090	>50	144.7	62.7	27.0	6.07	65.8	87.72	16.00	0.960
11292	11	25-38860	57	2.730	C.641	C.981	4.479	190.0	242.7	25.7	6.64	104.5	306.73	61.80	0.130
11315	11	26-40997	57	2.877	C.794	C.574	5.161	84.2	93.1	18.8	11.88	88.8	67.89	-2.53	0.637
11522	58	25-30891	58	1.252	C.895	C.136	2.447	326.5	93.1	44.8	12.11	58.5	304.35	-2.57	0.733
11531	6	25-35912	58	2.158	C.744	C.563	3.834	93.0	273.2	1.2	0.90	89.1	274.43	-24.88	0.388
11573	7	10-22160	58	4.047	C.752	1.003	7.092	194.3	106.4	27.4	-0.18	105.8	252.51	48.23	0.956
11589	7	10-24345	58	2.172	C.627	C.809	3.534	241.8	107.4	5.7	5.63	105.7	271.28	-10.78	0.729
11598	7	11-19742	58	1.415	C.507	C.699	2.138	265.8	108.3	24.6	15.40	84.2	290.63	18.67	0.808
11614	7	11-36369	58	2.221	C.566	C.965	3.477	210.8	108.4	127.6	0.70	29.8	357.20	30.56	0.796
11630	7	12-34857	58	1.444	C.508	C.133	2.756	325.7	109.4	44.5	11.90	59.5	318.60	1.05	0.843
11633	7	12-38123	58	3.242	C.823	C.251	6.233	324.8	109.4	67.5	11.10	60.2	317.06	10.55	0.924
11637	7	12-39300	58	-14.362	1.065	C.936	>50	329.0	289.4	179.7	0.01	9.84	27.40	11.09	0.484
11642	7	15-19792	58	-20.746	1.030	C.631	>50	255.4	112.1	114.2	3.61	43.0	338.65	24.76	0.336
11642	7	15-27757	58	54.770	C.982	C.978	>50	157.4	112.2	107.0	0.97	44.0	9.27	51.73	0.486
11653	7	21-33612	58	7.485	C.964	C.268	14.702	299.9	117.9	26.6	8.70	74.0	312.96	-2.03	0.825
11656	7	21-37599	58	4.854	C.806	C.941	8.767	146.5	118.0	135.9	0.78	26.6	26.23	37.48	0.694
11669	7	22-37881	58	3.065	C.978	C.068	6.062	152.6	299.9	30.5	7.44	61.6	333.72	-18.83	0.625
11670	7	22-39833	58	3.043	C.912	C.267	5.820	303.0	119.9	7.6	3.26	75.2	316.14	-11.70	0.656
11670	7	23-40314	58	3.571	C.875	C.445	6.697	281.3	119.9	0.9	0.50	85.0	307.37	-18.17	0.516
11672	7	23-42393	58	2.576	C.610	C.005	4.157	193.3	119.9	12.8	-0.29	128.8	243.23	26.65	0.065
11682	8	10-17310	58	1.269	C.226	C.983	1.555	213.3	136.9	77.2	2.56	117.3	275.24	21.84	0.982
11690	8	10-26747	58	10.355	C.909	C.948	19.843	149.7	137.0	110.6	1.37	41.5	43.78	58.57	0.410
11752	8	12-32778	58	5.343	C.898	C.952	17.734	150.7	139.0	113.6	1.22	35.6	46.18	57.21	0.580
11752	8	12-33182	58	-2.348	1.431	C.1013	>50	177.5	139.0	114.3	-0.12	41.0	30.06	56.56	0.704
11823	8	14-45582	58	6.320	C.850	C.945	11.696	148.6	141.0	112.3	1.35	40.1	49.59	58.31	0.841
11823	8	14-45582	58	-233.923	1.004	C.950	>50	151.1	141.0	111.3	1.33	41.6	49.61	59.73	0.831
11875	5	10-21377	58	2.603	C.903	C.252	4.934	125.5	346.9	1.3	0.56	74.5	3.32	0.53	0.611
11912	5	15-32680	58	2.356	C.926	C.176	4.537	195.8	351.8	4.9	1.83	69.9	12.82	2.82	0.864
11933	5	16-24730	58	-3.429	1.269	C.926	>50	210.8	172.7	162.2	0.32	15.2	69.44	32.61	0.257
11939	5	16-37000	58	5.029	C.951	C.440	17.619	278.9	172.8	20.0	9.5	83.8	353.20	15.98	0.925
11946	5	16-41619	58	10.616	C.905	C.1005	20.227	179.6	172.9	162.5	-0.01	10.2	82.36	33.43	0.803
11949	5	16-44622	58	22.905	C.963	C.854	44.956	226.1	172.9	146.9	0.90	23.3	63.70	39.74	0.966
11959	5	17-27362	58	2.681	C.644	C.956	4.407	209.0	172.9	146.9	1.21	40.3	64.50	41.31	0.564
12002	5	20-41195	58	25.592	C.974	C.669	>50	71.1	356.8	97.1	4.79	51.0	59.82	-14.84	0.570
12011	1C	8-41876	58	1.256	C.778	C.288	2.303	128.9	10.3	5.7	3.22	71.8	29.15	6.97	0.517
1204P	1C	8-43437	58	59.355	C.993	C.989	>50	191.6	134.5	146.8	0.23	19.8	104.54	42.28	0.853
1206C	1C	9-23594	58	1.669	C.714	C.477	2.861	284.7	195.3	2.7	2.00	83.5	19.86	11.86	0.865
12064	1C	9-27708	58	3.402	C.880	C.405	6.395	105.2	15.3	8.1	4.24	83.0	24.34	2.30	0.869
12066	1C	9-29418	58	2.060	C.639	C.743	3.376	250.0	195.4	40.8	13.27	80.0	358.53	6.29	0.869
12066	1C	9-29860	58	1.755	C.830	C.305	3.285	122.1	15.4	5.5	2.88	75.3	30.39	7.80	0.892
12075	1C	9-39421	58	1.684	C.786	C.360	3.008	116.9	15.5	5.2	3.22	77.6	28.47	6.41	0.920
12090	1C	10-12892	58	2.568	C.613	C.994	4.143	171.1	196.2	1.9	0.71	158.3	267.10	-1.75	0.775

Table 1 (Cont.)

Film	mo	day	yr	a	e	q	q'	$\omega$	$\Omega$	i	c.w.	$\lambda$	$\alpha^{\circ}$	$\delta^{\circ}$	CZ <sub>R</sub>
12093	IC	10.16503	58	2.385	0.559	0.957	3.822	207.2	196.2	46.1	5.75	81.4	311.56	75.21	0.725
12094	IC	10.15936	58	2.928	0.822	0.522	5.334	273.4	196.2	2.1	1.39	89.0	15.77	9.42	0.664
12095	IC	10.17415	58	2.168	0.592	0.884	3.453	46.3	16.2	5.2	5.39	117.4	355.89	-18.80	0.574
12096	IC	10.19130	58	2.944	0.701	0.880	5.007	224.5	196.3	20.3	1.13	98.9	333.05	48.34	0.955
12097	IC	10.20074	59	2.346	0.667	0.781	3.910	242.9	196.3	20.3	14.29	96.9	349.94	37.61	0.992
12111	IC	10.35266	58	-20.019	1.040	0.809	>50	231.1	196.4	167.8	0.36	17.3	91.53	30.07	0.712
12112	IC	10.36216	58	2.707	0.863	0.370	5.044	111.0	16.4	5.0	2.69	80.6	26.45	6.34	0.865
12114	IC	10.38007	58	1.222	0.673	0.600	2.045	119.1	16.4	0.1	0.07	76.2	29.05	11.77	0.885
12116	IC	10.40042	58	21.087	0.968	0.668	41.507	70.9	16.5	162.6	0.73	22.9	86.05	14.68	0.846
12119	IC	10.43241	58	-36.702	1.024	0.882	>50	219.7	196.5	128.2	1.36	32.6	93.01	52.55	0.892
12125	IC	15.20220	58	-10.403	1.063	0.652	>50	250.9	201.2	3.6	2.23	101.3	8.03	8.75	0.871
12127	IC	15.22555	58	2.325	0.574	0.990	3.660	191.2	201.2	9.8	4.04	135.8	300.48	22.09	0.616
12131	IC	15.26898	58	-0.866	0.574	0.990	3.660	191.2	201.3	9.2	8.97	66.3	39.25	31.99	0.931
12131	IC	15.41377	58	-141.505	1.004	0.444	1.288	313.9	201.3	163.0	0.80	25.0	89.70	15.20	0.890
12169	IC	17.33762	58	-7.173	1.100	0.721	>50	77.0	22.4	159.9	0.76	22.9	93.83	12.92	0.611
12173	IC	17.38247	58	166.818	0.996	0.671	>50	61.9	23.3	46.5	1.42	80.6	50.59	-29.20	0.469
12179	IC	17.44005	58	2.481	0.717	0.703	4.258	72.8	23.4	107.8	3.50	42.6	89.33	-12.08	0.699
12186	IC	18.21289	58	1.845	0.830	0.313	3.384	120.7	24.2	4.7	2.43	76.0	38.01	11.01	0.726
12189	IC	18.24527	58	2.368	0.782	0.517	4.220	95.5	24.2	21.5	11.71	83.7	37.98	-10.17	0.623
12201	IC	18.25881	58	2.271	0.776	0.509	4.033	276.8	204.2	4.6	3.26	87.1	24.06	15.99	0.946
12201	IC	18.37434	58	3.574	0.896	0.370	6.778	109.2	24.4	19.4	8.69	79.3	39.11	-0.86	0.803
12202	IC	18.38286	58	2.123	0.861	0.295	3.951	121.4	24.4	5.5	2.73	75.7	38.52	10.86	0.881
12210	IC	18.46350	58	5.034	0.813	0.940	9.128	29.1	24.4	160.9	0.30	13.5	107.33	11.66	0.884
12229	IC	20.46537	58	20.294	0.970	0.610	39.978	77.6	26.4	163.4	0.71	24.2	94.40	16.07	0.955
12231	IC	20.48749	58	-77.020	1.008	0.592	>50	258.9	206.5	164.5	0.81	31.0	95.72	45.81	0.985
12255	IC	21.34281	58	11.914	0.948	0.616	23.212	77.5	27.3	5.1	3.39	81.1	50.91	12.86	0.808
12317	IC	5.22096	58	1.698	0.744	0.434	2.961	108.5	42.2	4.4	2.76	82.3	50.45	13.63	0.371
12332	IC	6.10909	58	1.932	0.774	0.437	3.426	106.3	43.1	9.5	7.89	103.7	20.62	27.53	0.921
12336	IC	6.15530	58	3.642	0.794	0.750	6.534	243.3	223.1	13.7	12.23	107.0	1.94	43.16	0.982
12338	IC	6.16512	58	1.687	0.536	0.876	2.898	228.1	223.1	13.7	3.19	81.3	51.72	13.31	0.839
12343	IC	6.23139	58	2.161	0.812	0.407	3.915	108.4	43.2	5.5	5.57	117.9	301.46	43.91	0.420
12348	IC	6.24509	58	2.613	0.621	0.989	4.237	185.6	223.2	17.8	1.70	80.5	50.40	21.32	0.973
12348	IC	6.28737	58	2.156	0.824	0.387	4.005	290.5	223.2	3.0	0.81	24.3	95.29	15.77	0.770
12358	IC	21.36744	58	3.503	0.841	0.557	6.448	87.9	27.3	163.7	0.81	24.3	95.29	15.77	0.770
12395	IC	11.26502	58	-4.145	1.234	0.972	>50	194.9	48.2	7.1	4.16	82.7	55.77	12.48	0.912
12399	IC	10.30818	58	2.296	0.828	0.394	4.197	109.1	47.4	4.9	2.88	80.9	56.02	15.07	0.354
12407	IC	10.38860	58	4.352	0.845	0.673	8.031	252.4	237.4	18.1	1.71	94.8	41.35	43.52	0.904
12453	IC	20.32751	58	2.171	0.803	0.428	3.914	105.8	57.4	7.5	4.57	82.1	65.51	13.88	0.932
12454	IC	20.34307	58	-36.623	1.026	0.965	>50	344.2	58.5	148.6	0.36	18.9	149.35	-7.05	0.637
12471	IC	21.45090	58	1.254	0.914	0.108	2.399	149.8	75.6	25.2	8.03	60.0	106.74	12.91	0.940
12557	IC	8.36565	58	3.414	0.722	0.948	5.880	24.4	76.4	4.8	4.13	137.9	30.13	-5.87	0.763
12564	IC	9.13155	58	-116.715	1.002	0.186	>50	128.4	77.5	36.7	8.44	69.0	99.44	8.14	0.534
12577	IC	10.19523	58	2.410	0.869	0.316	4.505	117.4	77.6	13.0	5.92	76.1	92.15	13.71	0.943
12577	IC	10.34220	58	0.759	0.750	0.190	1.327	332.9	259.5	0.5	0.28	54.7	117.23	21.47	0.943
12627	IC	12.19545	58	1.244	0.883	0.146	2.342	324.8	259.5	23.7	8.14	62.1	111.63	33.08	0.573
12627	IC	12.29792	58	2.238	0.818	0.427	4.249	105.0	79.6	5.1	2.95	82.3	87.84	18.40	0.965
12636	IC	12.29792	58	1.558	0.929	0.142	3.853	321.0	262.5	26.7	7.74	64.8	111.93	32.99	0.421
12690	IC	15.15395	58	2.748	0.673	0.398	4.593	38.5	81.5	6.0	5.94	121.8	50.66	-0.08	0.804
12691	IC	14.15275	58	2.748	0.673	0.398	4.593	38.5	81.5	6.0	5.94	121.8	50.66	-0.08	0.804
12702	IC	14.27708	58	1.467	0.905	0.140	2.795	323.7	261.6	23.2	7.56	63.3	112.39	32.05	0.865
12706	IC	14.32037	58	1.400	0.897	0.144	2.655	323.6	261.7	23.4	7.87	63.1	112.76	32.41	0.954
12755	IC	2.24904	59	1.545	0.897	0.147	2.942	142.2	101.0	22.5	7.24	63.9	127.33	8.74	0.697
12797	IC	8.22500	59	1.746	0.443	0.972	2.520	15.6	107.1	9.1	5.79	128.3	57.79	-24.81	0.468
12843	IC	15.37645	59	4.553	0.851	0.740	9.165	242.6	294.3	134.8	1.67	29.7	194.32	19.22	0.656



Table 2. Meteor trajectory data from Super-Schmidt double-station photographs

$n_A$	$n_{ML}$	$H_A$	$H_{BEG}$	$H_B$	$H_{BEG}$	$H_{ML}$	$H_A$	$H_{BEND}$	$\sin Q$	$V_\infty$	$V_G$	$V_H$	Film
17	11	109.4	105.6	105.6	105.4	105.4	95.5	95.5	0.398	60.900	59.630	43.220	1806
14	2	51.7	58.5	51.6	51.7	51.6	51.1	51.1	0.341	36.400	34.950	34.540	2855
18	12	59.7	58.2	91.7	55.7	55.7	91.7	91.7	0.200	30.800	35.470	34.830	2855
18	12	100.2	101.4	100.2	100.2	100.2	92.5	92.7	0.610	30.800	28.590	38.680	9234
13	7	84.1	84.1	75.9	84.1	75.9	80.5	80.5	0.427	19.000	15.630	37.610	9285
38	3	86.9	86.9	75.5	86.9	75.5	82.4	82.4	0.622	19.570	16.570	37.560	9287
13	4	96.6	97.0	96.6	96.6	96.6	51.8	51.8	0.372	59.600	58.350	41.820	9298
22	12	114.6	112.1	114.6	110.1	114.6	104.8	104.8	0.033	63.300	61.950	39.950	9298
5	1	98.2	100.2	98.2	98.2	98.2	94.4	94.4	0.141	67.700	66.570	41.420	9299
40	32	96.4	96.3	96.4	96.4	96.4	83.2	82.3	0.384	27.360	25.060	23.420	9305
30	16	104.0	100.0	104.0	104.0	104.0	96.9	96.9	0.228	47.500	46.160	41.900	9308
14	7	82.0	80.5	82.0	82.0	82.0	78.6	78.6	0.799	14.600	9.490	29.960	9310
11	5	86.4	86.3	86.4	86.4	86.4	82.3	82.8	0.970	19.800	16.590	37.940	9311
17	6	90.0	89.3	90.0	90.0	90.0	82.0	81.3	0.958	29.200	27.010	35.990	9311
75	47	93.9	93.7	93.9	93.9	93.9	78.7	78.7	0.664	19.130	15.920	39.330	9311
21	15	88.6	88.5	88.6	88.6	88.6	79.3	80.1	0.210	24.700	22.160	36.620	9312
14	14	102.2	104.2	102.2	102.2	102.2	94.5	94.5	0.511	47.400	46.040	42.470	9317
60	8	86.0	95.1	86.0	86.0	86.0	80.4	80.4	0.056	20.400	17.520	38.790	9318
16	6	94.5	101.3	94.5	94.5	94.5	88.5	86.8	0.146	31.100	29.330	36.130	9319
24	16	111.1	109.0	111.1	111.1	111.1	99.6	97.7	0.111	62.000	60.660	41.460	9321
23	18	98.9	98.8	98.9	98.9	98.9	83.4	83.0	0.364	31.300	28.290	36.210	9327
23	21	102.7	103.3	102.7	102.7	102.7	96.4	86.8	0.131	34.900	33.110	36.680	9328
13	4	105.2	104.8	105.2	105.2	105.2	91.9	93.4	0.197	67.200	66.130	41.360	9333
17	7	104.5	103.0	104.5	104.5	104.5	97.8	94.2	0.068	68.600	67.540	42.910	9342
12	3	115.7	112.1	115.7	115.7	115.7	102.3	103.1	0.288	69.000	68.020	42.290	9343
58	40	98.7	94.9	98.7	98.7	98.7	80.2	79.5	0.080	25.590	23.370	35.120	9343
22	18	92.5	93.8	92.5	92.5	92.5	84.7	85.0	0.748	29.470	27.430	26.910	9345
22	9	96.6	96.4	96.6	96.6	96.6	78.0	82.1	0.971	17.500	13.640	38.140	9361
9	9	96.6	96.4	96.6	96.6	96.6	91.4	89.5	0.309	45.250	43.620	40.800	9363
26	27	102.9	102.0	102.9	102.9	102.9	81.2	81.5	0.523	19.100	15.780	38.990	9369
15	5	100.9	100.1	100.9	100.9	100.9	85.3	84.5	0.687	29.750	27.710	36.560	9371
19	10	59.4	100.4	59.4	59.4	59.4	85.9	90.4	0.170	44.300	42.730	41.630	9385
31	31	103.5	102.6	103.5	103.5	103.5	84.4	84.4	0.870	31.000	28.940	37.480	9396
15	13	86.4	86.5	86.4	86.4	86.4	79.2	78.9	0.467	31.200	28.140	37.360	9397
15	13	86.4	86.5	86.4	86.4	86.4	79.2	78.9	0.125	28.400	26.150	36.610	9398
16	5	95.8	102.4	95.8	95.8	95.8	86.0	87.7	0.234	30.500	28.430	37.110	9398
25	20	102.2	102.2	102.2	102.2	102.2	84.8	87.4	0.224	23.800	21.960	36.980	9400
19	15	93.7	95.9	93.7	93.7	93.7	83.9	84.1	0.574	26.900	24.700	36.990	9405
39	25	96.0	96.0	96.0	96.0	96.0	82.0	81.3	0.975	23.500	20.720	34.970	9411
13	4	89.1	84.4	89.1	89.1	89.1	86.1	82.4	0.043	14.600	9.440	28.980	9412
20	6	111.2	105.1	111.2	111.2	111.2	96.8	95.5	0.594	43.000	41.500	41.670	9413
15	5	111.6	110.9	111.6	111.6	111.6	96.8	94.4	0.298	66.000	65.090	41.470	9432
10	7	90.8	90.7	90.8	90.8	90.8	88.5	79.9	0.173	17.300	13.510	37.920	9438
6	1	76.8	75.5	76.8	74.2	74.2	74.3	74.3	0.179	11.500	3.320	29.670	9446
3	2	104.4	104.5	104.4	104.4	104.4	103.8	103.4	0.010	62.400	61.040	39.200	9447
7	5	107.1	105.4	107.1	107.1	107.1	103.2	103.2	0.202	69.000	58.860	41.380	9452
1	1	100.8	101.6	100.8	100.8	100.8	87.4	87.0	0.968	28.100	25.920	37.220	9466
1	1	116.5	116.6	116.5	116.5	116.5	105.3	110.8	0.176	59.100	67.950	40.610	9469
1	1	85.0	85.0	85.0	85.0	85.0	78.1	76.3	0.072	24.100	21.620	35.800	9472
21	17	107.1	107.1	107.1	107.1	107.1	96.8	96.4	0.958	62.300	61.310	42.340	9478
23	16	89.1	101.7	89.1	89.1	89.1	89.6	88.7	0.611	31.000	29.190	37.930	9487
5	5	85.5	104.3	85.5	85.5	85.5	87.1	86.9	0.744	30.100	28.240	37.380	9488
12	4	82.4	81.7	82.4	82.4	82.4	79.5	80.0	0.777	15.940	11.350	36.070	9491
49	31	93.7	94.1	93.7	93.7	93.7	84.1	84.2	0.422	18.100	14.180	38.060	9503
11	3	55.8	95.5	55.8	55.8	55.8	91.1	90.7	0.256	44.880	43.160	42.220	9503
46	35	103.6	103.6	103.6	103.6	103.6	82.6	82.6	0.278	32.000	28.780	39.590	9504
23	22	100.3	100.3	100.3	100.3	100.3	99.3	87.8	0.773	30.160	28.060	36.960	9511
64	40	90.5	90.1	90.5	90.5	90.5	82.2	81.9	0.164	19.040	15.750	39.500	9513
9	2	102.8	104.1	102.8	102.8	102.8	96.7	95.2	0.733	44.500	42.370	42.160	9521

Table 2. (Cont.)

$n_A$	$n_{ML}$	$H_{BEG}$	$H_{BEG}$	$H_{BEG}$	$H_{ML}$	$H_{A\_END}$	$H_{B\_END}$	$\sin Q$	$V_\infty$	$V_G$	$V_H$	Film
14	12	55.0	97.0	97.0	55.0	51.0	94.2	0.144	36.900	35.100	38.270	9522
16	6	91.4	91.4	91.4	91.4	84.6	84.6	0.591	22.000	18.910	36.350	9530
26	16	120.4	113.4	113.4	120.4	97.2	100.3	0.250	63.500	62.300	42.690	9542
17	5	67.8	61.7	61.7	67.8	64.1	61.0	0.523	34.900	32.920	24.620	9542
14	12	105.8	107.0	107.0	105.8	93.0	92.9	0.599	72.800	71.760	41.780	9548
28	13	90.1	89.6	89.6	90.1	88.3	88.3	0.640	29.430	27.120	35.330	9560
21	12	104.6	107.6	107.6	104.6	90.2	87.5	0.975	42.400	40.850	42.900	9564
26	12	53.4	50.9	50.9	53.4	42.4	42.4	0.988	26.200	23.750	37.160	9566
21	16	106.6	105.8	105.8	106.6	92.0	90.2	0.820	47.780	43.360	42.650	9568
16	10	104.2	101.1	101.1	104.2	94.4	91.1	0.755	37.700	36.100	41.230	9568
10	5	107.6	107.6	107.6	107.6	98.9	98.9	0.421	61.200	60.180	42.680	9578
25	15	101.0	100.0	100.0	101.0	98.1	98.0	0.968	33.400	33.610	42.610	9578
8	3	106.3	105.7	105.7	106.3	102.4	103.7	0.377	44.360	42.860	41.850	9579
13	6	105.4	105.3	105.3	105.4	98.8	98.2	0.213	43.710	42.560	42.440	9580
10	7	95.6	96.3	96.3	95.6	93.2	92.2	0.328	26.700	24.540	39.630	9581
8	3	52.5	54.1	54.1	52.5	91.2	91.1	0.220	31.400	29.690	37.380	9581
10	5	111.9	113.7	113.7	111.9	100.4	99.9	0.791	70.880	69.970	41.730	9584
12	3	55.1	100.0	100.0	55.1	91.3	91.5	0.106	60.500	59.220	41.380	9590
43	23	85.0	88.2	88.2	85.0	81.4	83.5	0.436	18.200	14.600	36.790	9590
8	3	94.3	94.3	94.3	94.3	90.2	86.8	0.186	39.100	37.720	33.500	9595
34	18	98.1	95.1	95.1	98.1	91.0	90.5	0.313	19.600	16.380	39.190	9596
25	5	93.6	92.6	92.6	93.6	86.1	83.8	0.328	26.150	24.000	38.350	9597
12	6	59.3	57.7	57.7	59.3	52.3	52.3	0.568	53.500	52.240	37.210	9597
27	22	53.2	53.3	53.3	53.2	49.4	49.4	0.028	33.300	31.140	31.050	9606
12	6	82.6	82.9	82.9	82.6	79.5	77.3	0.967	16.300	12.060	37.220	9606
21	11	55.9	101.4	101.4	55.9	87.8	86.2	0.880	36.800	34.990	34.400	9612
19	12	103.5	101.7	101.7	103.5	92.9	92.2	0.737	36.070	34.260	33.860	9615
20	13	108.5	107.9	107.9	108.5	83.0	82.7	0.583	17.330	13.460	34.750	9616
11	3	108.8	108.8	108.8	108.8	100.1	100.5	0.507	69.110	67.960	42.220	9618
16	7	102.0	103.8	103.8	102.0	91.0	90.5	0.935	36.600	34.920	34.420	9621
29	27	118.7	118.8	118.8	118.7	98.9	98.8	0.423	72.900	71.770	41.900	9623
11	6	111.7	111.9	111.9	111.7	100.9	98.2	0.970	68.000	64.960	42.810	9624
23	15	100.2	100.2	100.2	100.2	85.8	86.0	0.939	36.050	34.440	34.090	9629
14	4	112.4	111.7	111.7	112.4	105.1	105.4	0.101	54.700	53.340	41.100	9634
16	12	98.2	99.4	99.4	98.2	88.7	87.6	0.598	35.650	33.910	33.570	9638
16	11	97.7	98.0	98.0	97.7	88.5	87.8	0.911	36.000	34.340	34.050	9641
35	32	97.8	105.0	105.0	97.8	78.2	84.5	0.051	37.600	36.010	35.390	9658
21	15	99.4	95.1	95.1	99.4	85.8	85.9	0.566	36.300	34.640	34.310	9658
15	5	100.1	98.8	98.8	100.1	89.3	90.1	0.476	41.400	40.010	37.440	9659
23	13	104.3	104.0	104.0	104.3	89.8	88.7	0.098	36.700	35.090	34.360	9660
4	2	95.4	93.8	93.8	95.4	92.9	92.2	0.028	36.750	35.210	36.290	9660
11	7	95.9	101.2	101.2	95.9	92.2	92.4	0.446	51.000	49.880	45.090	9660
27	21	95.6	99.0	99.0	95.6	84.5	84.5	0.669	33.600	33.940	33.650	9661
24	14	102.6	102.9	102.9	102.6	87.1	85.7	0.323	41.600	40.240	39.430	9661
23	16	100.0	100.1	100.1	100.0	82.9	84.7	0.559	35.970	34.460	34.110	9671
31	15	100.2	100.4	100.4	100.2	85.9	86.6	0.428	36.500	35.020	34.570	9671
12	6	102.5	104.4	104.4	102.5	97.7	97.3	0.237	42.500	40.770	40.980	9671
22	13	113.1	113.2	113.2	113.1	97.3	96.5	0.154	58.800	57.940	40.320	9672
20	16	114.5	115.1	115.1	114.5	103.1	104.2	0.345	66.600	65.610	41.670	9672
21	5	83.2	83.7	83.7	83.2	79.2	78.9	0.500	13.860	7.820	25.740	9673
21	18	115.6	108.7	108.7	115.6	103.8	104.6	0.221	70.000	68.830	42.210	9675
29	23	98.9	102.0	102.0	98.9	83.0	83.4	0.595	36.300	34.720	34.300	9675
15	6	111.3	111.0	111.0	111.3	100.6	100.9	0.119	52.640	51.260	41.410	9684
23	21	118.6	117.5	117.5	118.6	96.8	96.7	0.576	70.150	69.080	42.180	9684
51	14	77.5	78.5	78.5	77.5	67.2	67.0	0.537	14.600	9.720	38.180	9688
15	7	103.8	104.3	104.3	103.8	100.4	99.0	0.289	35.000	33.190	40.430	9698
28	11	95.5	95.4	95.4	95.5	86.8	85.7	0.417	31.700	29.600	39.270	9700
13	3	76.9	77.4	77.4	76.9	76.2	74.8	0.524	12.710	6.010	31.130	9705
48	36	94.5	97.0	97.0	94.5	82.0	81.6	0.655	21.100	18.000	38.560	9705
9	3	76.2	78.1	78.1	76.2	75.4	76.0	0.590	12.400	5.530	31.820	9707

Table 2. (Cont.)

$n_A$	$n_{ML}$	$H_A$	$BEG$	$H_B$	$BEG$	$H_{ML}$	$H_A$	$BEND$	$H_B$	$BEND$	$\sin Q$	$V_\infty$	$V_G$	$V_H$	Film
13	7	111.2	112.5	111.3	100.8	98.2	0.476	61.800	60.680	41.370	9723				
10	5	84.0	84.1	84.0	80.2	80.6	0.912	24.900	22.450	36.050	9723				
26	16	91.7	91.0	78.9	78.2	0.920	26.800	26.470	37.060	9727					
46	20	96.7	96.5	96.7	85.9	90.0	0.297	26.850	24.400	38.030	9731				
48	20	101.5	101.7	75.9	80.0	0.607	28.300	26.040	37.150	9732					
50	22	91.6	91.9	81.6	80.2	0.162	16.000	11.870	37.200	9734					
6	2	84.8	87.7	84.8	82.8	82.4	0.472	23.700	21.060	38.840	9737				
6	1	90.2	92.6	87.5	85.2	0.611	28.000	25.730	32.260	9737					
30	22	97.4	98.0	84.8	86.0	0.558	25.500	23.140	37.200	9739					
21	10	115.4	115.2	101.2	101.2	0.260	70.800	69.620	41.520	9744					
23	16	105.3	105.8	92.8	92.3	0.668	42.550	41.540	41.800	9768					
14	10	83.3	83.4	80.4	80.8	0.428	16.000	11.710	33.610	9774					
26	22	105.8	105.3	94.8	91.8	0.318	33.500	31.770	42.200	9780					
21	2	90.1	90.3	85.0	85.1	0.110	19.700	16.710	35.890	9781					
21	6	125.2	121.2	103.2	103.2	0.025	64.700	63.680	40.250	9784					
11	4	95.5	94.8	89.6	89.6	0.141	42.000	40.770	36.020	9784					
25	16	114.2	115.1	98.6	99.1	0.337	65.840	65.040	42.040	9787					
22	6	96.9	96.9	87.4	87.1	0.112	49.340	47.780	41.710	9794					
42	22	92.2	92.2	75.9	74.1	0.877	25.200	22.800	27.100	9814					
17	11	74.1	73.6	74.1	69.9	0.427	11.300	1.870	31.440	9826					
22	14	91.4	93.0	86.6	92.4	0.423	24.100	21.080	38.630	9831					
32	22	97.4	96.6	86.6	92.4	0.124	33.500	31.680	37.760	9833					
46	42	104.5	104.5	94.2	91.7	0.046	42.200	40.340	37.920	9833					
22	13	82.3	86.0	82.3	76.0	0.692	16.310	12.070	38.300	9841					
12	3	76.9	77.0	75.3	74.4	0.600	12.000	4.470	31.720	9851					
32	17	98.0	96.8	87.3	87.0	0.466	24.090	21.350	40.620	9857					
30	3	87.7	86.5	75.1	75.8	0.578	26.880	22.140	38.600	9883					
16	2	114.8	116.9	106.3	106.1	0.330	72.600	71.580	42.330	9901					
15	2	55.9	108.1	101.8	101.8	0.279	48.600	47.070	40.470	9920					
19	12	106.8	101.9	95.2	95.2	0.310	70.500	69.330	40.690	9923					
21	11	105.9	108.2	98.4	98.4	0.321	53.600	52.130	42.670	9934					
21	5	93.0	92.6	83.0	82.4	0.867	27.000	24.600	26.170	9934					
14	1	88.2	88.7	88.2	84.0	0.630	19.500	16.220	32.160	9952					
12	2	90.3	100.1	94.1	93.4	0.188	36.800	35.410	35.180	9958					
15	10	55.5	59.3	91.0	89.7	0.503	39.700	38.100	36.380	10001					
11	2	80.5	80.7	80.5	77.7	0.346	13.500	7.700	33.910	10002					
17	11	104.9	102.8	104.9	88.8	0.751	59.610	58.570	41.590	10007					
9	4	82.2	82.5	80.1	80.2	0.452	17.000	13.050	35.620	10029					
8	8	85.6	86.9	84.7	81.8	0.636	13.300	7.680	37.540	10032					
19	13	94.3	91.6	84.2	85.7	0.652	17.600	13.620	37.360	10039					
20	12	100.0	100.2	95.5	95.6	0.273	41.100	39.200	37.050	10061					
13	2	84.4	85.1	84.4	80.0	0.201	16.400	12.270	32.390	10075					
28	17	110.8	107.8	110.8	99.7	0.357	61.500	60.450	39.270	10082					
17	6	89.1	88.6	89.1	83.5	0.921	20.800	17.750	36.900	10111					
7	1	92.6	95.6	89.6	89.1	0.281	30.600	28.570	36.430	10111					
10	2	98.2	98.8	92.2	95.6	0.020	48.800	47.180	39.900	10111					
15	10	112.0	111.5	98.5	98.6	0.400	67.000	65.890	42.190	10116					
26	16	101.4	101.8	101.4	89.0	0.352	40.750	39.380	37.140	10118					
42	32	101.7	100.4	101.7	84.5	0.487	28.910	26.560	38.160	10176					
25	22	93.3	96.1	82.3	83.2	0.612	21.300	18.030	33.620	10188					
22	9	59.3	99.9	88.4	87.9	0.473	38.400	36.770	37.790	10198					
9	7	117.0	111.8	105.6	100.7	0.157	54.000	52.320	44.670	10244					
12	2	88.0	93.6	82.5	86.6	0.061	37.000	35.080	37.460	10244					
13	9	91.8	92.1	87.4	86.1	0.079	34.000	32.410	37.810	10245					
11	3	85.5	91.9	85.5	86.8	0.059	25.500	23.250	39.850	10254					
62	36	86.7	86.7	104.2	103.1	0.142	63.500	62.200	42.310	10257					
7	2	110.3	108.3	110.3	105.5	0.405	64.200	63.080	41.050	10265					
21	7	113.5	112.0	113.5	102.9	0.139	67.600	66.350	41.940	10270					
18	2	86.0	85.0	86.0	82.9	0.148	19.440	16.340	35.160	10270					

Table 2. (Cont.)

$n_A$	$n_{ML}$	$H_A$	$H_{BEG}$	$H_B$	$H_{BEG}$	$H_{ML}$	$H_A$	$H_{END}$	$H_B$	$H_{END}$	$\sin Q$	$V_\infty$	$V_G$	$V_H$	Film
3	1	101.5	101.5	101.5	101.5	101.5	59.3	58.8	0.228	55.040	53.680	40.070	10273		
13	7	86.8	86.8	86.8	86.8	86.8	23.3	21.9	0.887	18.200	14.590	35.430	10332		
15	2	84.5	84.5	84.5	84.5	84.5	80.5	79.6	0.951	19.100	15.480	32.080	10335		
18	4	52.7	52.7	52.7	52.7	52.7	86.5	85.0	0.951	27.100	24.630	41.120	10404		
22	16	95.8	95.8	95.8	95.8	95.8	86.9	86.1	0.302	45.000	47.490	40.790	10516		
21	15	112.4	112.4	112.4	112.4	112.4	102.0	103.9	0.066	47.000	45.470	41.510	10518		
11	6	87.2	87.2	87.2	87.2	87.2	85.1	85.0	0.763	24.830	22.210	38.220	10551		
22	5	93.8	93.8	93.8	93.8	93.8	83.9	84.9	0.224	35.300	33.700	38.220	10562		
11	10	107.6	107.6	107.6	107.6	107.6	98.0	97.3	0.481	69.500	68.350	41.070	10564		
49	35	103.1	103.1	103.1	103.1	103.1	78.1	80.1	0.653	33.400	31.450	41.770	10569		
7	1	81.8	81.8	81.8	81.8	81.8	80.5	80.0	0.593	13.600	8.050	32.500	10571		
19	10	111.9	111.9	111.9	111.9	111.9	97.2	97.8	0.925	68.770	67.650	41.150	10608		
18	5	86.3	86.6	86.6	86.3	83.9	83.9	84.9	0.183	18.700	15.420	36.370	10773		
37	26	95.6	90.5				82.0	82.9	0.165	20.400	17.270	37.510	10781		
42	35	102.6	101.2				87.7	86.0	0.876	28.100	25.950	38.120	10785		
28	23	89.6	89.6				81.8	84.4	0.918	20.600	17.590	36.180	10785		
26	23	98.1	97.8				83.0	86.2	0.120	31.850	29.970	36.180	10786		
30	18	101.3	98.7				85.6	89.3	0.323	37.460	35.970	36.150	10793		
15	4	107.2	107.7				98.2	98.6	0.814	48.000	46.680	39.460	10802		
8	5	106.8	109.1				98.6	99.8	0.218	70.600	69.540	43.190	10804		
30	15	105.1	102.9				94.4	95.1	0.062	33.000	31.330	37.930	10808		
15	15	75.6	74.9				72.7	71.1	0.973	11.550	2.660	26.880	10824		
23	12	88.1	88.2				84.3	85.6	0.282	19.400	16.170	31.620	10825		
12	6	112.1	110.8				100.6	101.0	0.389	68.100	67.010	39.150	10825		
12	1	83.0	86.0				78.9	83.1	0.956	20.200	17.090	24.920	10828		
8	6	107.8	109.1				100.9	101.3	0.328	69.900	68.760	42.100	10829		
26	72	101.4	100.6				81.2	83.2	0.992	19.740	16.310	38.260	10849		
80	72	101.4	100.6				81.2	83.2	0.810	27.200	24.520	35.980	10874		
35	35	79.8	79.4				70.5	75.5	0.805	13.000	9.910	29.350	10877		
26	5	55.0	85.6				85.4	84.5	0.776	14.800	9.910	29.350	10890		
24	7	92.8	102.1				83.4	83.4	0.986	30.200	28.140	35.450	10893		
48	26	97.4	96.4				87.9	88.2	0.541	68.400	67.180	41.430	10894		
22	1	52.8	93.1				83.9	84.5	0.572	30.700	28.260	35.230	10905		
24	7	92.0	91.5				86.2	86.4	0.936	34.900	32.910	38.850	10939		
27	18	98.3	98.1				87.1	85.8	0.747	23.200	20.620	38.900	10947		
8	4	108.3	109.1				98.8	99.6	0.721	33.000	31.280	38.390	10951		
12	2	86.0	86.3				82.1	82.9	0.363	64.700	63.660	42.040	10956		
8	0	86.0	86.9				86.7	86.7	0.917	26.000	23.400	36.940	10980		
17	1	94.4	91.0				84.1	83.6	0.984	21.000	17.960	37.510	10982		
15	12	112.2	117.2				96.3	98.2	0.843	27.500	25.360	39.390	10988		
43	3	97.3	100.9				83.9	83.8	0.742	23.500	20.570	38.590	11003		
43	3	96.6	100.9				79.6	79.7	0.942	26.630	24.170	41.360	11006		
18	5	91.5	91.5				87.5	88.1	0.836	31.700	29.460	34.580	11007		
11	1	86.7	87.0				83.5	84.1	0.837	21.000	17.930	34.580	11015		
19	6	88.0	88.4				80.8	83.3	0.429	24.870	22.400	37.580	11015		
14	10	117.1	107.9				102.7	102.6	0.946	71.800	70.750	41.200	11035		
15	15	92.1	90.5				86.3	88.1	0.123	30.400	28.650	38.500	11037		
15	15	92.5	93.1				86.0	86.2	0.973	21.590	18.590	33.180	11040		
9	6	111.8	111.6				104.3	102.8	0.547	69.000	67.840	41.750	11042		
24	8	78.8	78.8				85.4	85.3	0.993	33.600	31.770	35.930	11042		
13	80	101.1	98.4				76.8	76.9	0.382	12.400	6.180	33.590	11044		
14	4	101.1	98.4				89.0	87.4	0.360	57.000	56.040	42.470	11052		
26	20	105.0	106.0				94.1	91.9	0.530	43.310	41.990	38.820	11052		
15	5	97.8	96.2				92.7	90.4	0.169	32.000	30.330	37.440	11052		
50	18	105.8	105.9				93.0	92.5	0.739	38.900	37.340	41.740	11075		
24	14	102.4	101.9				90.4	91.8	0.889	37.000	35.250	36.020	11075		
11	10	101.9	102.4				95.2	95.1	0.934	40.500	38.840	41.500	11093		
33	25	94.7	95.4				82.6	81.9	0.710	23.400	20.680	38.690	11093		
13	3	109.7	112.2				100.9	99.9	0.763	67.500	66.280	42.860	11096		

Table 2. (Cont.)

$n_A$	$n_{ML}$	$H_A$	$H_{BEG}$	$H_B$	$H_{BEG}$	$H_{ML}$	$H_A$	$H_{END}$	$H_B$	$H_{END}$	$\sin Q$	$V_\infty$	$V_G$	$V_H$	Film
43		84.2	92.2				70.6	70.3			0.907	15.600	11.070	38.110	11111
40		87.6	85.0				76.9	75.9			1.000	15.500	11.120	37.470	11111
17		97.3	96.7				87.4	86.6			0.820	28.900	27.570	26.510	11113
4	2	111.1	111.8			111.1	107.9	106.5			0.558	65.300	64.070	39.410	11123
12	E	112.2	113.6			112.2	101.2	106.3			0.553	68.000	66.890	42.270	11127
14		59.1	101.1				87.3	86.4			0.998	20.700	17.550	38.760	11182
9		75.9	79.4				78.1	77.9			0.559	14.800	5.950	34.090	11201
24	14	51.4	95.8			91.4	80.5	84.1			0.936	21.600	18.670	42.250	11207
34	30	95.6	97.9			95.6	90.5	80.3			0.389	32.100	29.960	39.070	11208
10		98.9	98.9				97.3	96.9			0.758	22.400	19.650	38.800	11213
23		105.1	104.8				90.8	90.4			0.756	41.550	39.910	41.590	11215
41		96.7	100.4				75.9	85.4			0.887	27.300	25.050	37.600	11221
26	15	111.1	111.3			111.1	95.5	94.2			0.175	66.900	65.670	40.430	11224
16	5	95.3	95.7			95.3	89.5	89.2			0.859	28.200	23.620	37.490	11227
26		95.7	98.8				83.1	82.5			0.561	26.000	23.490	37.200	11256
6	4	94.1	95.0			94.1	90.5	88.6			0.211	36.800	34.910	33.490	11282
48	26	105.2	105.3			105.2	97.0	96.7			0.193	64.200	62.860	33.500	11284
23	25	89.7	97.4			89.7	78.1	88.5			0.930	24.000	21.360	39.210	11284
15	11	104.8	105.7			104.8	93.7	94.2			0.529	46.200	44.870	42.620	11290
26		54.2	93.9				89.3	88.8			0.707	20.450	17.280	38.350	11292
41	3	88.2	88.6			88.2	76.1	78.0			0.531	26.760	24.610	38.570	11315
21	14	97.0	95.3			97.0	87.3	87.1			0.774	37.900	36.060	32.520	11522
35	26	52.9	91.5			92.9	86.4	86.7			0.175	24.800	22.410	36.610	11531
45	31	94.4	93.4			94.4	78.7	81.9			0.987	22.000	19.030	39.040	11573
13	3	83.4	83.5			83.4	80.2	81.1			0.980	18.900	15.280	36.540	11589
21	10	87.2	86.8			87.2	76.6	78.3			0.797	22.500	19.330	33.450	11598
14	7	109.5	111.2			109.5	98.1	98.7			0.574	60.300	59.040	36.660	11614
17	10	98.2	99.1			98.2	89.1	88.5			0.980	38.670	36.980	33.610	11630
8	6	91.5	92.5			91.5	84.2	83.1			0.845	44.600	43.230	38.340	11633
17	13	98.6	106.0			98.6	85.8	88.4			0.485	72.250	71.050	42.480	11634
21	14	100.1	100.4			100.1	92.9	95.6			0.152	60.000	58.610	42.260	11637
19	12	111.8	111.6			111.8	102.6	103.1			0.271	58.600	57.300	41.560	11642
18	16	100.2	103.3			100.2	90.7	90.6			0.933	38.500	36.870	40.320	11653
13	10	108.1	114.2			108.1	98.5	97.7			0.524	64.700	63.480	39.520	11656
22	11	98.0	97.0			98.0	88.1	89.8			0.760	43.400	41.960	38.150	11659
34	31	97.3	98.1			97.3	84.1	84.5			0.547	34.620	32.940	38.120	11670
12	5	89.3	89.8			89.3	86.1	85.8			0.625	29.800	27.870	38.680	11670
22	6	84.6	84.8			84.6	82.8	82.8			0.810	15.500	11.280	37.420	11672
9	4	77.2	78.8			77.2	75.5	75.3			0.987	12.500	5.730	32.410	11682
23	20	110.4	109.2			110.4	100.9	105.5			0.161	59.100	57.850	40.780	11690
15	6	109.6	108.3			109.6	100.9	98.5			0.241	60.000	58.760	40.670	11752
14	13	107.2	109.3			107.2	96.7	97.8			0.584	65.200	64.070	46.110	11752
5	5	106.1	108.0			106.1	101.9	100.7			0.462	59.000	57.850	40.120	11823
15	5	111.6	111.3			111.6	99.2	98.2			0.924	60.200	59.070	41.870	11823
10	5	89.2	85.9			89.2	85.6	83.3			0.658	34.600	32.490	37.680	11875
35	31	107.2	105.7			107.2	88.7	88.4			0.960	36.650	34.880	37.230	11912
6	0	120.0	122.9			120.0	118.1	118.3			0.049	74.000	72.840	44.950	11933
26	15	101.4	102.3			101.4	88.2	89.4			0.981	33.200	31.410	40.800	11939
10	5	112.5	115.7			112.5	102.9	103.6			0.156	70.900	69.800	40.980	11946
8	6	106.8	114.3			106.8	98.0	99.1			0.592	68.000	67.010	41.520	11949
27	21	113.1	114.2			113.1	97.1	97.8			0.417	56.500	55.220	37.850	11959
7	4	108.8	109.1			108.8	105.1	102.9			0.720	54.500	53.240	41.600	12002
35	6	98.9	98.1			98.9	85.9	89.7			0.703	28.800	26.240	32.980	12011
25	20	120.3	122.6			120.3	95.3	109.5			0.530	69.800	68.740	41.940	12048
42	33	95.2	97.2			95.2	80.1	84.9			0.964	25.200	22.460	35.260	12060
20	4	89.7	89.7			89.7	81.2	79.5			0.883	31.000	28.850	38.910	12064
12		89.0	89.2			89.0	84.0	78.6			0.591	29.200	27.080	36.660	12066
27	20	97.5	101.6			97.5	95.3	84.9			0.932	30.800	28.650	35.790	12066
40	37	55.2	96.3			55.2	79.7	91.3			0.431	28.400	26.310	35.330	12075
24	E	68.8	89.2			68.8	76.7	78.3			0.510	13.700	8.460	37.810	12090

Table 2. (Cont.)

$n_A$	$n_{ML}$	$H_A$	$H_{BEG}$	$H_{BEG}$	$H_{ML}$	$H_A^{END}$	$H_B^{END}$	$\sin \Omega$	$V_\infty$	$V_G$	$V_H$	Film
4	4	88.2	101.4	101.4	102.9	95.0	84.4	1.000	29.700	27.580	37.470	12091
18	4	102.5	104.8	104.8	103.7	85.1	84.7	0.852	27.250	24.600	38.370	12092
18	5	83.7	84.0	84.0	83.7	90.5	90.1	0.967	16.490	12.030	38.960	12094
18	5	91.2	55.8	55.8	90.7	84.3	84.3	0.987	22.800	19.960	38.390	12096
18	180	85.5	85.3	85.3	26.7	77.1	74.9	0.719	22.200	19.200	37.380	12097
12	5	106.8	110.1	108.8	108.8	98.8	59.0	0.397	71.300	70.160	42.650	12111
12	5	84.0	83.5	83.5	84.0	73.6	74.2	0.975	30.900	28.950	38.050	12112
39	23	55.4	52.7	95.4	95.4	81.4	80.7	0.691	24.100	21.540	32.400	12116
7	7	115.7	118.9	115.7	115.7	98.3	54.9	0.820	68.500	67.410	41.630	12116
14	6	118.2	125.8	118.2	118.2	105.1	100.2	0.230	65.400	64.350	42.420	12119
14	2	89.3	92.1	85.3	92.1	81.2	81.2	0.820	28.200	25.800	43.160	12125
38	23	78.2	77.3	78.2	78.2	71.5	72.0	0.736	14.420	9.610	37.370	12127
39	10	84.5	89.6	84.5	84.5	73.9	77.1	0.987	18.200	14.260	27.460	12131
17	12	114.0	115.0	114.0	114.0	96.8	55.1	0.708	68.400	67.350	42.240	12149
12	5	110.8	116.7	110.8	110.8	105.0	103.8	0.483	70.700	69.520	43.610	12169
13	13	105.0	105.0	105.0	105.0	98.2	97.3	0.605	36.600	34.920	42.110	12173
15	7	106.3	106.8	106.3	106.3	96.6	95.4	0.944	55.000	53.800	37.700	12179
36	36	103.2	102.6	103.2	103.2	85.0	84.7	0.906	30.900	28.580	38.050	12186
44	35	97.0	97.5	97.0	97.0	82.7	82.5	0.723	28.500	26.050	37.480	12189
21	15	85.4	92.1	85.4	85.4	76.0	77.0	0.158	26.300	23.770	37.270	12210
21	15	100.4	96.7	100.4	100.4	86.2	85.3	0.584	33.150	31.350	39.130	12210
32	32	100.5	98.9	100.5	100.5	85.3	85.0	0.657	32.000	30.150	36.900	12202
13	13	109.8	109.4	109.8	109.8	96.5	96.1	0.953	69.500	68.450	40.040	12210
14	11	113.9	112.9	113.9	113.9	98.8	97.9	0.901	68.000	67.060	41.670	12229
21	15	117.0	115.8	117.0	117.0	94.3	54.2	0.760	65.900	64.990	42.330	12231
14	14	111.1	112.1	111.1	111.1	102.6	103.0	0.900	68.000	66.810	41.300	12253
24	14	96.4	96.7	96.4	96.4	87.9	86.9	0.964	26.800	24.180	35.570	12317
54	54	55.7	100.7	55.7	89.4	87.4	87.4	0.335	27.730	25.030	38.460	12332
22	22	92.5	94.4	92.5	92.5	83.5	82.7	0.995	22.300	19.180	39.390	12336
17	6	85.9	85.4	85.9	85.9	81.1	80.6	0.755	17.400	13.390	36.310	12338
23	23	104.2	104.2	104.2	104.2	85.9	85.7	0.596	29.150	26.770	37.120	12343
40	40	83.3	82.8	83.3	79.2	79.6	79.6	0.883	17.000	13.220	38.060	12348
10	3	86.2	86.8	86.3	81.6	81.6	81.6	0.903	29.600	27.390	37.210	12348
6	3	111.2	111.3	111.3	105.4	100.3	100.3	0.859	65.500	64.310	39.080	12358
10	3	96.5	102.0	96.5	84.6	84.5	84.5	0.595	29.000	26.690	37.620	12395
27	27	112.2	122.8	112.2	103.2	104.7	104.7	0.047	71.000	70.630	44.760	12399
33	33	59.7	100.7	59.7	80.8	81.6	81.6	0.772	29.500	27.510	37.470	12407
10	4	88.2	87.6	88.2	84.2	83.0	83.0	0.944	26.000	23.660	39.080	12453
47	47	90.9	90.5	90.9	70.9	71.2	71.2	0.309	28.500	26.330	37.220	12454
9	4	100.6	102.2	100.6	94.1	93.4	93.4	0.819	71.100	70.020	42.640	12471
14	4	89.2	89.1	89.2	80.6	81.7	81.7	0.298	36.950	35.220	43.050	12537
27	24	85.4	89.5	85.4	81.6	81.3	81.3	0.671	15.800	11.150	39.410	12544
25	22	104.9	105.8	104.5	90.9	91.0	91.0	0.704	44.300	42.560	42.510	12564
40	30	98.1	98.8	98.1	77.8	78.4	78.4	0.286	32.560	31.060	37.840	12577
31	31	94.2	95.5	94.2	87.4	87.6	87.6	0.489	25.000	22.030	25.140	12627
31	31	98.5	100.2	98.5	87.2	87.1	87.1	0.514	35.450	33.960	32.980	12627
60	60	94.6	94.9	94.6	74.2	70.2	70.2	0.587	29.100	26.860	37.700	12634
28	28	105.9	108.7	105.9	93.0	92.2	92.2	0.187	39.400	37.480	36.040	12630
23	23	90.7	89.1	90.7	83.0	85.6	85.6	0.789	16.900	12.610	38.440	12691
16	16	55.4	97.5	55.4	87.6	88.5	88.5	1.000	37.000	35.100	34.590	12702
31	31	99.4	99.9	99.4	74.6	75.3	75.3	0.623	36.400	34.550	34.170	12706
21	21	95.2	95.3	95.2	86.1	85.9	85.9	0.861	37.300	35.350	35.050	12755
21	21	87.4	88.4	87.4	82.0	82.0	82.0	0.442	13.700	8.240	35.980	12797
19	19	108.5	110.5	108.5	104.9	103.6	103.6	0.455	64.900	63.650	40.280	12843

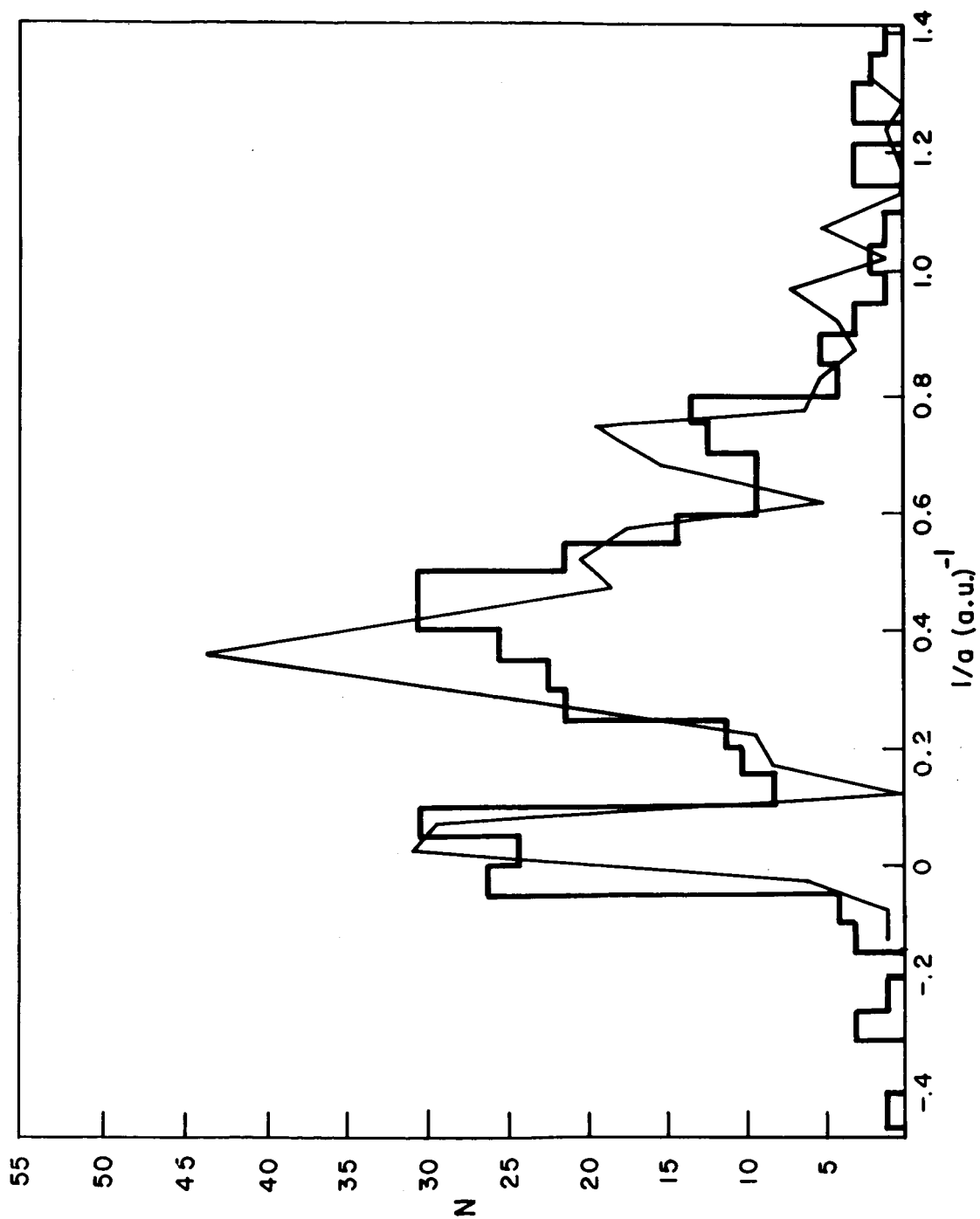


Figure 1. Distribution of meteor orbits in reciprocal semimajor axis.  
Line plot: Hawkins and Southworth (1961).

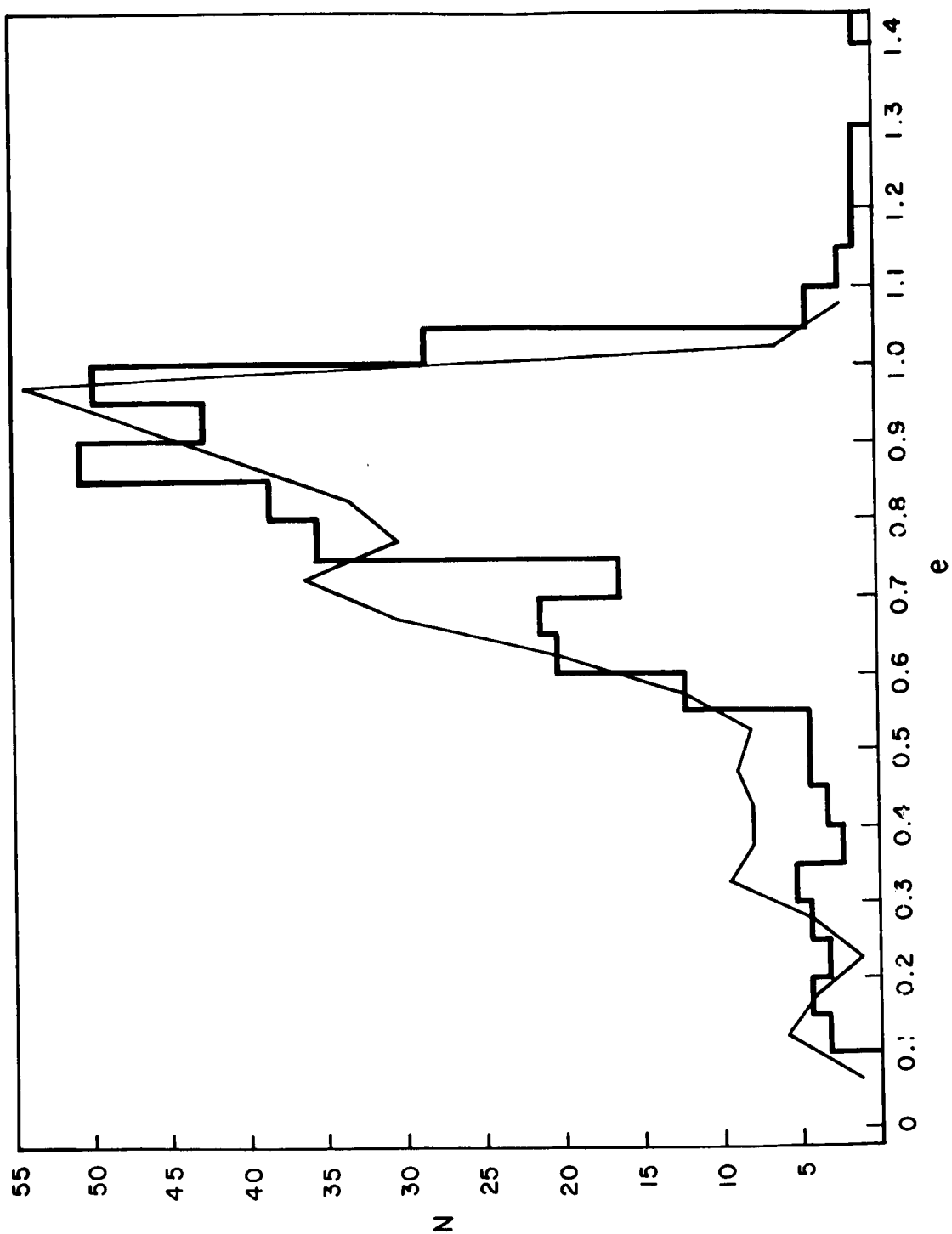


Figure 2. Distribution of meteor orbits in eccentricity.  
Line plot: Hawkins and Southworth (1961).



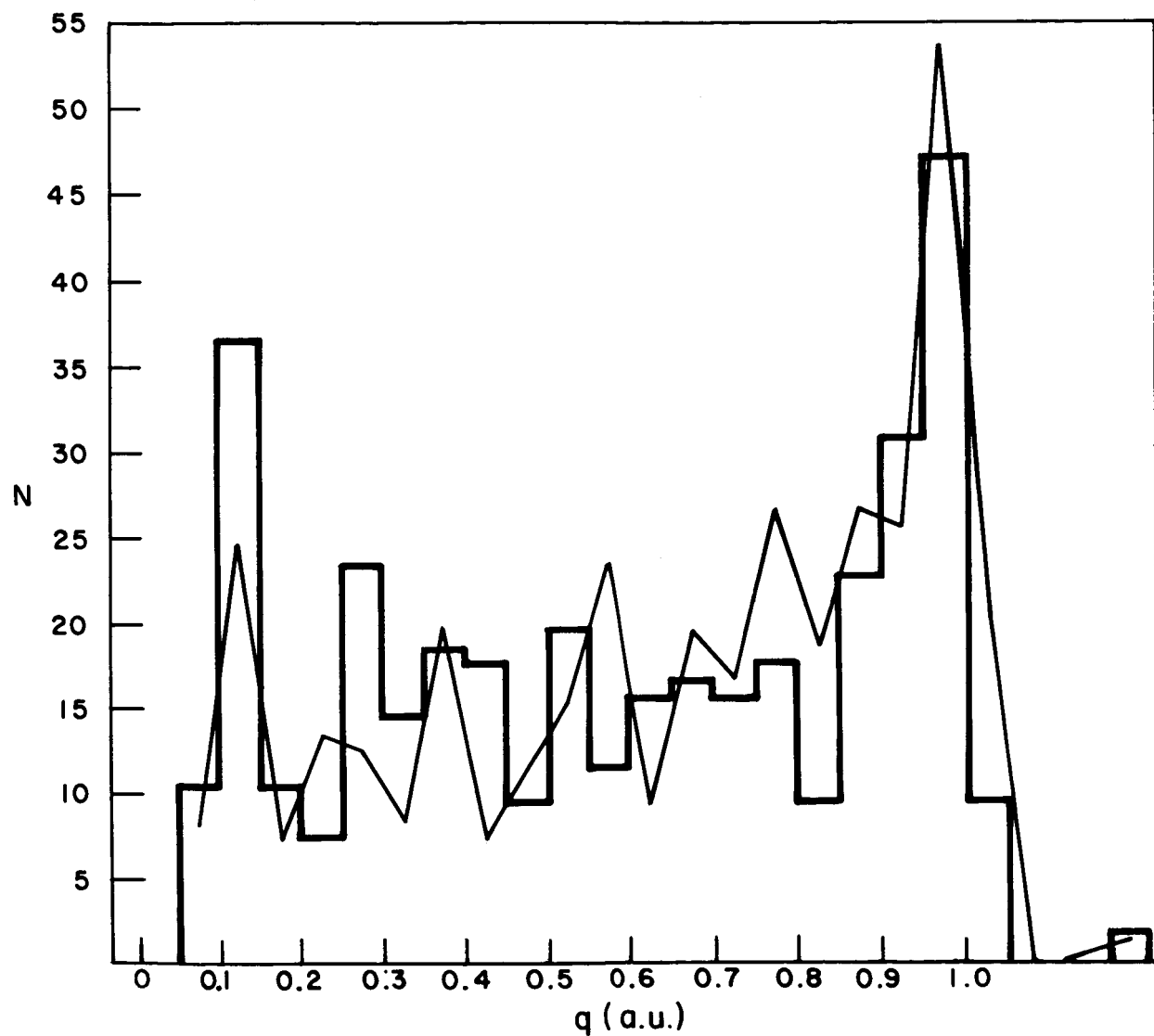


Figure 3. Distribution of meteor orbits in perihelion distance.  
Line plot: Hawkins and Southworth (1961).

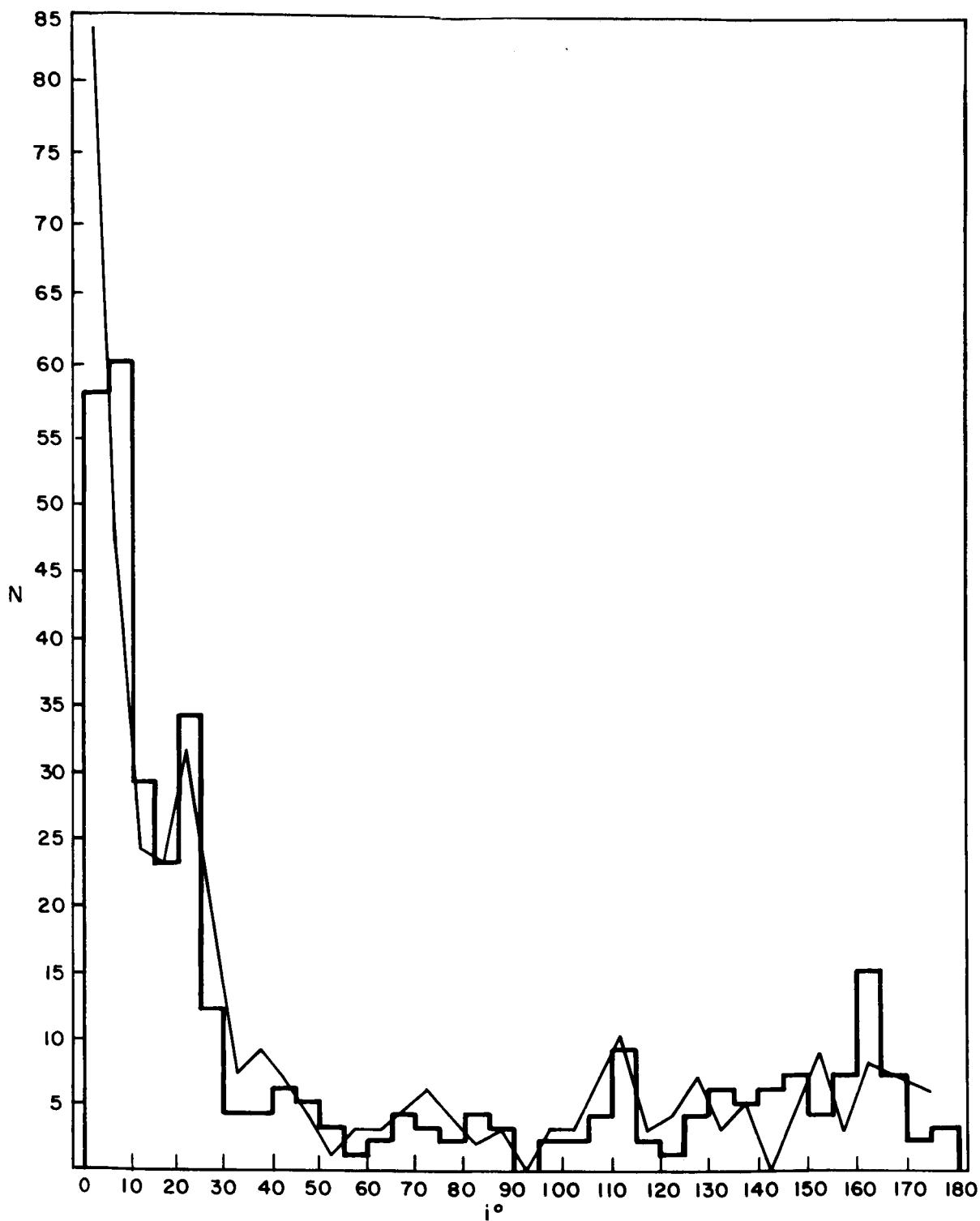


Figure 4. Distribution of meteor orbits in inclination.  
Line plot: Hawkins and Southworth (1961).

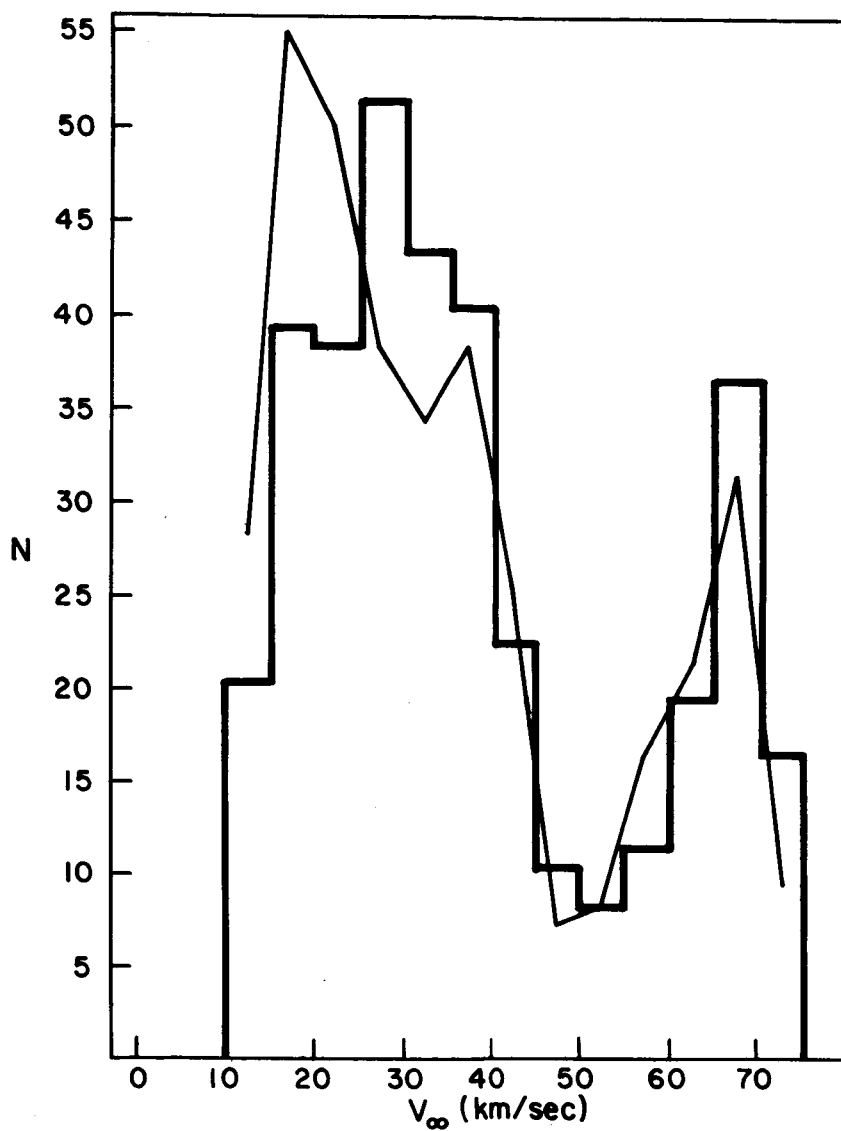


Figure 5. Distribution of meteor velocities.  
Line plot: Hawkins and Southworth (1961).

## 5. REFERENCES

HAWKINS, G. S. , AND SOUTHWORTH, R. B.

1961. Orbital elements of meteors. Smithsonian Contr. Astrophys. ,  
vol. 4, pp. 85-95.

JACCHIA, L. J. , AND WHIPPLE, F. L.

1961. Precision orbits of 413 photographic meteors. Smithsonian  
Contr. Astrophys. , vol. 4, pp. 97-129.

McCROSKY, R. E. , AND POSEN, A.

1961. Orbital elements of photographic meteors. Smithsonian Contr.  
Astrophys. , vol. 4, pp. 15-84.

STAFF, SMITHSONIAN ASTROPHYSICAL OBSERVATORY

1966. Smithsonian Astrophysical Observatory Star Catalog.  
Smithsonian Institution, Washington, D C.

WAGNER, A.

1963. A computer program for automatic star identification. BRL  
Memorandum No. 1535, 33 pp.

WHIPPLE, F. L

1954. Photographic meteor orbits and their distribution in space.  
Astron. Journ. , vol. 59, pp. 201-217.

WHIPPLE, F. L. , AND JACCHIA, L. J.

1957. Reduction methods for photographic meteor trails. Smithsonian  
Contr. Astrophys. , vol. 1, pp. 183-206.

## APPENDIX A

There is in the Super-Schmidt camera a focus post, which is photographed as a shadow on the periphery of the film. The line joining this marker (N) to the plate center defines the center-North Pole direction. The position of the shutter center on the film is well-defined. The observer records the approximate ( $\pm 5^\circ$ ) direction of the camera axis when he sets the position circles of the camera at the beginning of each exposure.

A gnomonic projection is used in copying the spherical Super-Schmidt films onto flat glass plates. Angles are preserved at C, the center of projection. Distances along a radial direction  $r$  transform into angular separation in the sky, according to  $\theta = \tan^{-1} r/f$ , where  $f$  is the focal length of the camera. Thus, we can plot the center of the field, the north direction, and the position of the star relative to these on a representation of the celestial sphere. See Figures A-1 through A-3.

Applying spherical trigonometry, we can compute for the unknown star (\*),  $90 - \delta_*$  and  $\Delta\alpha_*$ . The sign of  $\Delta\alpha_*$  is determined by the right- or left-handedness of the set NC\*.

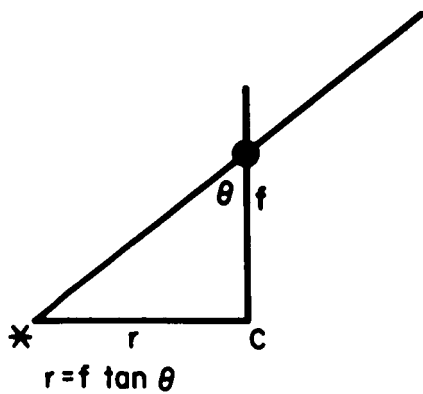


Figure A-1. In the camera.

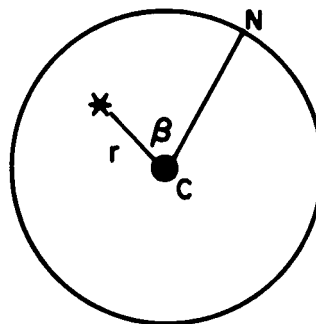


Figure A-2. On the film.

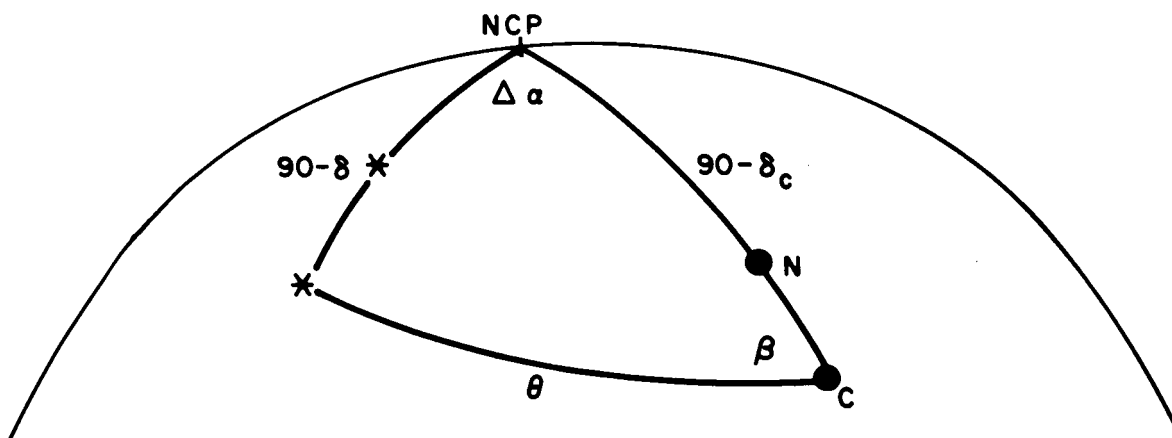


Figure A-3. In the sky.

## APPENDIX B

Given the measured plate coordinates and the sky coordinates of three to six bright stars, as well as the plate coordinates of the center, one can solve the set of equations,

$$\lambda_* \lambda_c + \mu_* \mu_c + \nu_* \nu_c = \cos \theta_* ,$$

where  $\lambda_*$ ,  $\mu_*$ ,  $\nu_*$  are direction cosines representing the spherical coordinates of the stars; the  $\theta_*$  are angular separations of the stars from the center as computed from their radial distances and from the focal length of the camera; and  $\lambda_c$ ,  $\mu_c$ ,  $\nu_c$  are the required direction cosines representing the spherical coordinates of the center.

A measure of the success of the fit can be obtained by comparing the  $\cos \theta$  computed from the new center coordinates with the input  $\cos \theta_*$ .

A further check should be made by comparing the plate-constants fit referred to the new center with that referred to the original input center.

## APPENDIX C

The basic data computed for the trajectory are the distances from some zero point for each time segment along the trail.

The form of the relation between distance and time is assumed to be

$$D = a + bt + ce^{kt} ,$$

where  $b$  is identified with the no-atmosphere velocity,  $V_{\infty} = (dD/dt)_{t = -\infty}$ , and  $ck^2e^{kt}$  with deceleration of the body.

The so-called "retardation curve" (see Fig. C-1) is a plot of

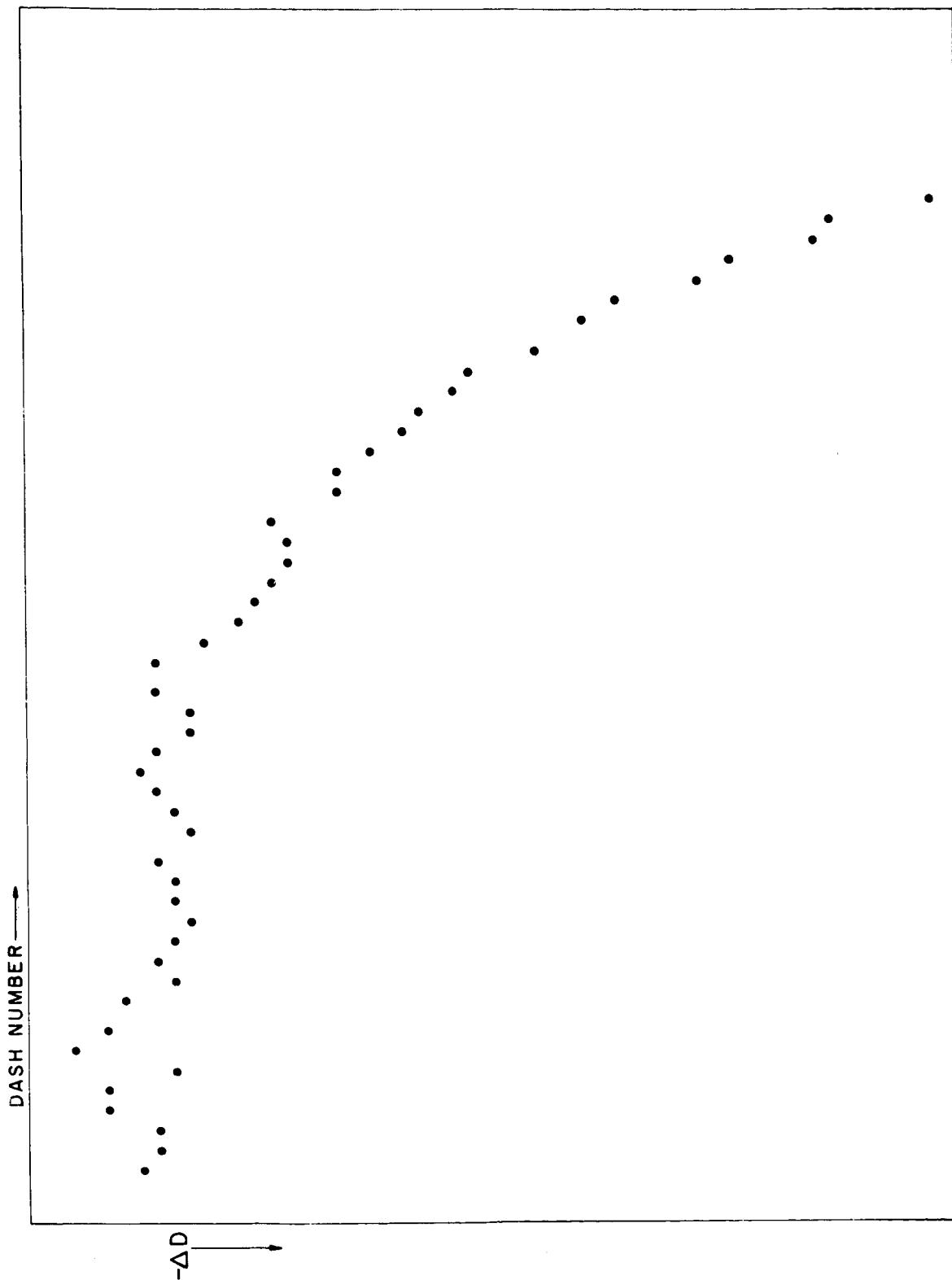
$$\Delta D = (D - D_0) - V_b(t - t_0) ,$$

where the subscript 0 refers to the first measured dash on this plate, and  $V_b$  is a mean beginning velocity computed from  $\Delta D/\Delta t$  for the first several dashes.

There is a departure from the method outlined in Whipple and Jacchia (1957). The search for  $k$  is made by machine, not by drawing a smooth curve by eye. From a given starting value, a search is initiated for a  $k$  for which a least-squares fit to  $a$ ,  $b$ , and  $c$  produces a minimum rms deviation.

The minimum is, in practice, very shallow and broad, and often oscillatory. This is not entirely satisfactory. However, the critical quantities  $b$  and  $dV/dt$  are relatively stable.





## APPENDIX D

### THE METHOD IN DETAIL

Films are selected in a convenient batch size from the library of 6000 pairs. They are examined, appropriately paired, and marked for copying onto glass plates. While they are being copied, the time and region data are transcribed and punched into cards. The glass plates are further marked to guide the measurer when the plate is on the measuring engine. A convenient morning's or afternoon's measuring is gathered for a sitting. A man can easily prepare in the morning the three or four plates that he can comfortably measure in the afternoon; the number depends on the quality of the images, the lengths of the trails, and related factors.

The original observers' records contain data on the approximate center of the field, the beginning time of the exposure, and the time of any visual event. The measurer, while preparing his films, must extract these data. He must establish that a mate exists, and then collect all the pertinent information. He marks the spherical film for the photographer so that the projection onto a flat plate by the copying camera has optimum density and focus in the region of the meteor. He then marks the plates for identification of points to be measured other than along the trail: the north point, shutter center, projection center, and six bright stars.

The initial division of the computer program is as follows:

A. Read in "library" data:

up to a total of 25 stations' coordinate cards;

up to a total of 25 precession matrix cards;

bright star map, list, and key.

B. Process each pair:

Identify station by film number.

Extract precession constants appropriate to year of meteor.

Compute sidereal time corresponding to input LST

Take means of repeated measures.

Identify the nature of each measure by a code on its card.

Compute effective  $(HA)_c$  by applying the time lapse between the exposure beginning and the meteor time, and the displacement of the projection center from the shutter center on the plate.

Compute predicted sky coordinates for each bright star, one plate at a time, and its corresponding grid number.

Search the nine grid positions of the map centered at this point and accumulate possibilities.

If fewer than four stars are matched with possible positions, displace the center by  $2^\circ$  and try again (four times).

If at least four stars are picked up, proceed to extract from the list precise corresponding positions.

Compute a plate-to-sky coordinate transformation for pairs of these stars two-by-two, selecting for each solution the set of the other star positions that gives the "best fit," discarding individual stars with deviations  $>50\mu$ , or solutions with mean deviations greater than this.

Select the best fit, and use these stars as the basis for a least-squares plate-constants solution.

If no satisfactory fit exists, move the center and try new predictions where the center is allowed to move by  $2^\circ$  in each coordinate  $(\alpha, \delta)$ .

If the effective focal length from this solution is satisfactory (within 3.5% of the accepted value), use these stars to compute an improved position of the projection center (Appendix B).

With this new center, perform a new least-squares plate-constants computation for use to predict sky coordinates of the measured faint stars.

Compute the grid codewords corresponding to these positions, and attach the plate number and star number to them.

Write on a scratch tape the plate identification, direction cosines of center and standard plate coordinate axes, focal length, plate coordinates of faint stars and trail dashes, and precession constants.

Compute relative station coordinates of the pair.

Write on tape for use in trajectory computation: all date and time information, station coordinates, camera and shutter information, and trail measures for the pair.

- C. Order the list of predicted positions for faint stars for all 20 pairs of the batch by declination and codeword to correspond to the catalog order.

Read in three records of faint-star map at a time flanking the next  $\delta$  of interest, and extract codewords of occupied grid positions surrounding the predicted positions.

Sort again on  $\delta$  and codeword.

- D. Read the faint-star list, degree by degree, and extract positions for the stars picked up from the map.

Order the entire batch on plate number and star number.

- E. Do the following for each plate:

Read in the data previously written on the scratch tape.

Set up the faint-star measures with the corresponding possible star positions.

Perform trial plate-constants solutions and sort out valid identifications as for bright stars.

Apply precession.

Compute a fit to the field-correction curve.

Apply field corrections, according to this curve, to the trail measures.

Compute constants for a least-squares straight line through both corrected and uncorrected trails.

Produce reference plots to help judge the success of these curve-fitting operations.

- F. Write on tape for use in the trajectory computation: plate constants, trail measures altered by the field corrections, and constants for equation of line with and without field corrections.

At this point, the computer program terminates. For sample output, see pages 42 through 44. The two tapes for further processing are saved. The output to date is examined. One must consider: Were there any failures of plates to proceed to this point? Do the plate-constants solutions indeed look reasonable? Does application of the computed field correction improve the appearance (straightness) of the trail? Are there scattered trail measures that unrealistically affect the determination of the trail equation? (Computer plots of field correction and of trails are provided for perusal.)

Having decided which pairs warrant continued processing, prepare the following input to the next programmed section:

- a. In the order of the previous section, one card for each plate, with the film number in the first eight columns, and a tag on those cards for plates for which the computed field correction should be omitted.
- b. The two data tapes prepared by the first programmed section.

The second program proceeds with a standard meteor-trajectory computation. For sample output, see page 45.

These data are now checked for inner consistency, for reliability of the solution for velocity and deceleration, and for any atypical behavior.

A "best" no-atmosphere velocity is computed to be used as input to the orbit computation.

The input to the orbit-computation program consists of the following:

- a. card "2" punched by the trajectory program, with  $V_{\infty}$  inserted, and
- b. card "1" punched by the star-identification program.

# Sample output from initial computer run.

DIRECTION COSINES OF PLATE CENTRE AND AXES  
 -0.666035C  
 -0.5713959  
 0.6396558  
 0.3455038  
 CENTRE  
 EXI AXIS  
 ETA AXIS

## PLATE CONSTANTS AND INVERSES

205.341234 -7.556333 898.205215 -7.124273 -206.137558 118.095469  
 0.00486375 -C.00017828 -4.34759647 -0.00016809 -0.00484496 C.72215271

## EFFECTIVE FOCAL LENGTH 205.5

L	M	N	X	Y	DX	DY	EXI	ETA
-0.85807C	-C.4328C7	0.276394	853.322	157.039	0.045	-C.004	-C.225C27	-0.181121
-C.836C07	-C.445932	0.319745	858.687	147.360	0.0C4	-C.00C	-C.197403	-C.135141
-C.746844	-C.615818	0.240934	899.739	164.812	-0.054	C.009	-C.001326	-0.226628
-0.585932	-C.785757	0.185750	949.929	174.384	0.045	-C.004	C.241754	-0.281396

plate constants  
 4 bright stars identified

DIRECTION COSINES OF PLATE CENTRE AND AXES  
 -C.6743515  
 -0.5831527  
 0.6541069  
 0.3426285  
 CENTRE  
 EXI AXIS  
 ETA AXIS

## PLATE CONSTANTS AND INVERSES

205.122145 -9.216458 901.786484 -7.922633 -205.040838 117.384525  
 0.00486669 -C.00021875 -4.36304110 -0.00018805 -0.00486862 C.741C7824

## EFFECTIVE FOCAL LENGTH 205.3

L	M	N	X	Y	DX	DY	EXI	ETA
-C.85807C	-C.4328C7	0.276394	853.322	157.039	-0.014	-C.015	-C.244599	-0.183872
-0.836C07	-C.445932	0.319745	858.687	147.360	-0.0C2	-C.002	-C.216317	-0.137826
-C.746844	-C.615818	0.240934	899.739	164.812	0.029	C.032	-C.020205	-0.230685
-0.585932	-C.785757	0.185750	949.929	174.384	-0.014	-C.016	C.221762	-0.286484

plate constants with  
 newly computed center  
 direction

## PREDICTIONS OF FAINT STARS

209.7316 9.5041  
 21C.2121 5.7579  
 210.2660 8.3210  
 211.6568 7.5622  
 212.6C5C 1C.0478  
 214.4664 8.7642  
 215.4594 8.2588  
 215.914C 9.3953  
 217.8111 8.4941  
 218.3932 9.9383  
 219.09C3 8.C752  
 219.833C 11.8702  
 219.978C 11.2761  
 220.5441 1C.9603  
 22C.74C5 1C.7947

SL 10C31.

DIRECTION COSINES OF PLATE CENTRE AND AXES

-0.6749547	-0.5820972	0.4534302	CENTRE
0.6530938	-0.7572770	0.	EXI AXIS
0.3433722	0.2961325	0.8912918	ETA AXIS

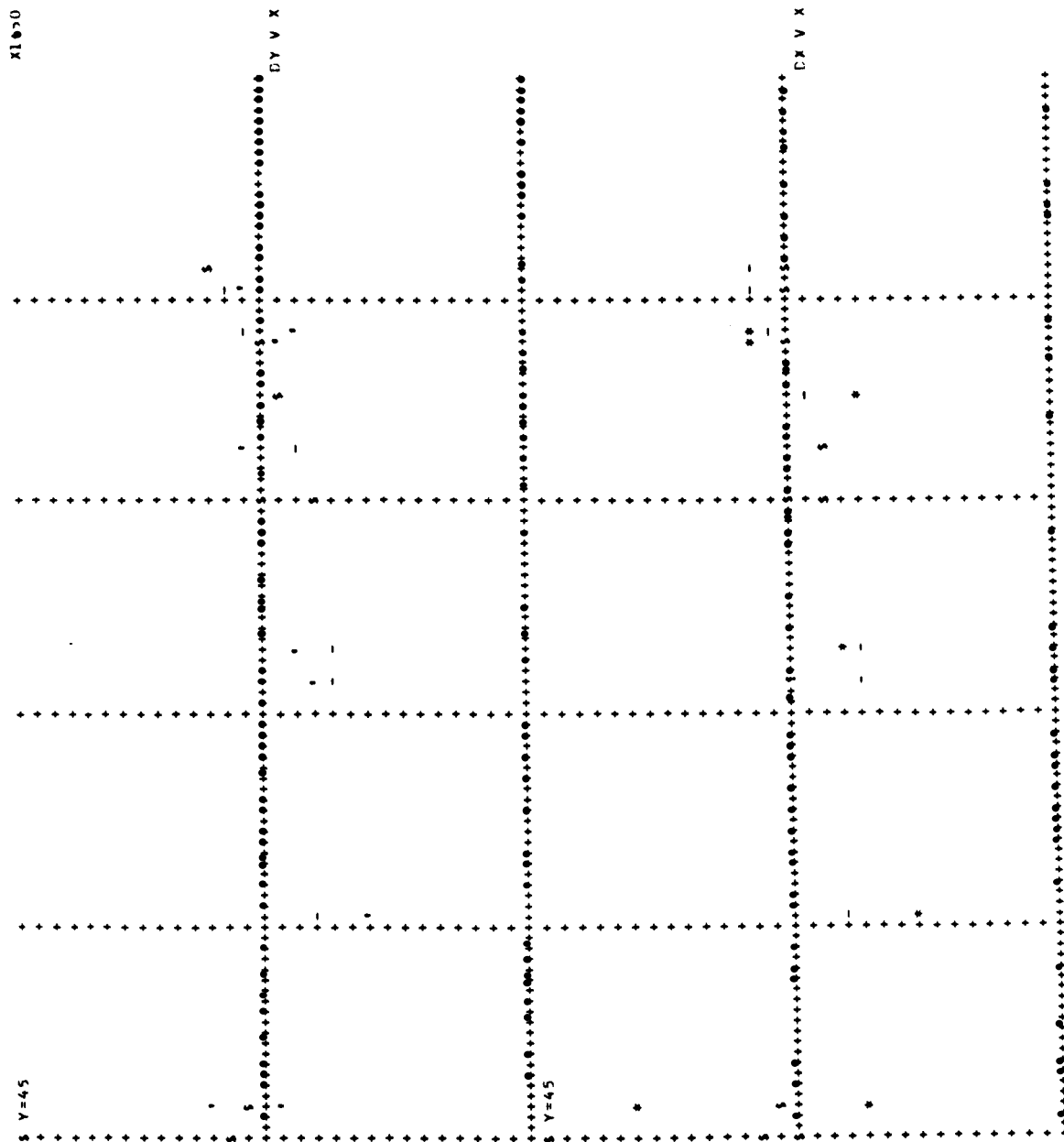
PLATE CONSTANTS AND INVERSES

205.480854	-9.387212	901.793777	-8.189466	-207.678612	116.685278
0.00485788	-C.0021958	-4.35518616	-0.00019156	-0.00480647	C.73359469

EFFECTIVE FOCAL LENGTH 205.7

L	M	N	X	Y	DX	DY	EXI	ETA	plate constants for 13 faint stars identified
-C.856413	-0.487851	0.166319	863.032	182.666	0.000	C.008	-C.262792	-0.369750	
-C.852177	-C.494636	0.170675	864.911	181.641	-0.011	-C.003	-C.193489	-0.305127	
-0.855036	-0.497547	0.166152	864.888	187.421	0.029	C.012	-C.194681	-0.332980	
-0.830096	-0.529243	0.175623	873.999	180.408	-0.019	-C.015	-C.149103	-0.300878	
-C.806759	-0.572785	0.145110	884.671	187.327	0.002	-C.008	-C.098684	-0.336219	
-C.799743	-0.577381	0.164445	886.362	182.761	-0.006	-C.004	-C.089506	-0.314613	
-0.782135	-0.605020	0.149048	893.498	186.145	0.001	C.001	-C.055546	-0.332272	
-C.772819	-0.610421	0.173597	895.531	180.372	-0.005	C.004	-C.044436	-0.364926	
-C.765299	-0.622932	0.141899	898.334	187.663	-0.009	-C.003	-C.032437	-0.340474	
-0.752354	-0.625628	0.206285	900.569	172.708	0.008	-C.003	-0.018212	-0.269023	
-0.752351	-0.628850	0.196257	901.183	174.976	0.008	-C.003	-0.015727	-0.280043	
-0.746940	-0.636904	0.190879	903.299	176.122	0.002	C.003	-C.005730	-0.285984	
-0.745174	-0.635810	0.188036	904.046	176.736	0.001	C.012	-C.002243	-0.289122	

plot of deviations from  
least-squares plate-  
constants fit  
DY vs X  
DX vs X  
where --- represent  
the fitted field  
correction curves





# Sample output of trajectory program.

plate	{ X	893.580	899.863	905.460	911.534	918.082
measure	{ Y	180.973	181.010	181.042	181.076	181.116
standard plate	{ EX1	-0.088245	-0.037891	-0.030855	-0.001511	0.030124
coordinates	{ ET1	-0.302059	-0.308715	-0.314644	-0.321079	-0.328017
direction cosines	{ EL	-0.964584	-0.956945	-0.949637	-0.940558	-0.930167
of 5 measured	{ EM	-0.258496	-0.286511	-0.311241	-0.337784	-0.365982
trail points	{ EN	0.052522	0.046557	0.041212	0.035389	0.029104
	RANGE	120.458	113.634	108.254	103.051	98.077
	COS Z	0.837918	0.840929	0.842987	0.844554	0.845468
earth curv. and elev.	{ DM	2.347	2.305	2.275	2.249	2.225
	HI	103.281	97.864	93.532	89.281	85.147
rectangular equat.	{ M EL	-116.192	-108.742	-102.781	-96.925	-91.228
coord. relative	{ N EL	-31.138	-32.557	-33.693	-34.809	-35.894
to the station	{ R EN	6.327	5.290	4.461	3.647	2.854
along the trail from	{ U	0.	7.655	13.779	19.796	25.649
point of greatest H						
	POLE	6.148785	0.987027	0.101664	-0.180589	0.978290
	LENGTH	8.699495			6.607906	
	SA+SB	17.601634			-12.921826	
	TIME	3.661997			3.667114	
	JU	35855.443252				
RELATIVE STATION CU-UKUS		23.401	-24.402	11.056		
	THE RADIANT					
					0.243789	
SIN Z					0.702286	
COS Z						
DIR-COS					0.135377	
a°, b°						
					169.2124	7.7804